ANALYSIS OF THE FACTORS AFFECTING IONOSPHERIC TOTAL ELECTRON CONTENT IN EAST AFRICA AND MIDDLE EAST

By

Mulu Eshetu

A THESIS SUBMITTED IN PARTIAL FULFILLMENT OF THE
REQUIREMENTS FOR THE DEGREE OF
MASTER OF SCIENCE IN SPACE PHYSICS
AT
ADDIS ABABA UNIVERSITY
SCHOOL OF GRADUATE STUDIES
ADDIS ABABA, ETHIOPIA

NOVEMBER, 2021

ADDIS ABABA UNIVERSITY

SCHOOL OF GRADUATE STUDIES

DEPARTMENT OF PHYSICS

The undersigned hereby certify that they have read and recommend to the school of graduate studies for acceptance a thesis entitled " **ANALYSIS OF THE FACTORS AFFECTING IONOSPHERIC TOTAL ELECTRON CONTENT IN EAST AFRICA AND MIDDLE EAST"** by **Mulu Eshetu** in partial fulfillment of the requirements for the degree of **Master of Science in**

Space Physics.

Dated: *November*, 2021

Approved by the Examination Committee: —

1. Advisor: Dr. Yitagesu Elfagd ——————-
2. Examiner: Dr. Gemechu Fanta ——————
3. Examiner: Dr. Girum Abebe ——————-
4. Chairwoman: Dr. Newayemedhin Aberra ——————

ADDIS ABABA UNIVERSITY

Date: **November, 2021**

Author: **Mulu Eshetu**

Title: **ANALYSIS OF THE FACTORS AFFECTING IONOSPHERIC TOTAL ELECTRON CONTENT IN EAST AFRICA AND MIDDLE EAST**

Department: **Physics**

Degree: **M.Sc** Convocation: **November** Year: **2021**

Permission is herewith granted to Addis Ababa University to circulate and to have copied for non-commercial purposes, at its discretion, the above title upon the request of individuals or institutions.

_____

Signature of Author

Contents

ACKNOWLEDGEMENT

First and foremost, I thank the Almighty God with his mother Saint Mariam, for blessed me with the finest of life's offering.

My thesis would not have been possible without the help of many people. First of all, I feel indebted of thankfulness to Dr. Yitagesu Elfagd, my master's thesis advisor for his continuous and enthusiastic support. Besides from my advisor, I would like to express my deepest gratitude to my mother, her love and prayers for me have kept me going this far.

I would like to express my deepest gratitude to give special thanks to my husband Tefera Mengstie for his love, care, kindness, support and encourage for all good and difficult times I had. My sincere thanks also goes to Tsilat Adinew for her help in facilitating my thesis; her advice and guidance carried me through all stages of the work.

I am extending my thanks to Semahegn Abayneh for his support with Matlab program installation and ongoing guidance. I would also like to express my sincere thanks to Alemayehu Mengesha, Assistant Professor of Space Physics (from IGSSA), for his intelligent comments and suggestions.

Last but not least, thanks to to my classmates for their support, encouragement, and all of the fun we have had over the past two years.

Abstract

The low latitude and equatorial ionospheric total electron content (TEC) variations are investigated using dual frequency GPS TEC data taken from 7 GPS stations in which 6 are found in East Africa and one is found in Saudi Arabia in the year of 2015. This GPS TEC data was used to study the diurnal, seasonal, geomagnetic and latitudinal variations of ionospheric TEC at these GPS stations as insufficient research results of ionospheric variations are available for these areas. The results of the analysis showed that the ionospheric TEC undergoes diurnal, seasonal, geomagnetic (quiet and disturbed day) and latitudinal variations. With regard to the diurnal variation, the TEC value shows minimum at predawn and gradual increase with time of the day attaining a maximum in the afternoon and a gradual decrease after sunset. This is the result of photo ionization of the atmosphere due to the increased intensity of solar radiation during day. On the other hand during night electron loss processes (ion-electron recombination and electron attachment) dominate and the TEC value is decreased. The TEC value in March shows a very rapid decrease after sunset due to the high recombination rate that is proportional to the square of the high electron density in March. Moreover, the night time TEC value shows a secondary minima maxima near dawn which may be due to the Counter Electrojet (CEJ). The TEC value in the solstice months of June and December don't show plateau and secondary maxima. It simply increase till noon and then decreases slowly during afternoon and during night.

The seasonal variation is caused by the relative position of the Earth with the sun which changes the solar zenith angle. The greatest TEC value occurred in the equinoctial month of March and the least occurred during the winter solstice month of December and intermediate TEC value is recorded in summer solstice month of June. The effects of geomagnetic storms on TEC values have been also considered in this study. The result reveals that the storm day TEC value is greater than the quiet day TEC value. This is due to the fact that high amount of solar particles reach

the earth and there is more ionization during the storm period. The TEC value also vary with latitude. The highest TEC value is obtained for stations that are closer to the geomagnetic equator (MOIU in Kenya) in the southern hemisphere. This may be the result of the occurrence of highly radiation of the sun and the DEBK station in Ethiopia located around EIA crest region is due to the fountain effect. The least value of TEC is observed for stations far from the geomagnetic equator (SOLA in Saudi Arabia) which is located beyond the EIA region. Moreover, TEC value of January 3, 2015 (at perihelion) is greater than that of the July 3, 2015 (aphelion), 2015. For the future more research need on the perihelion and aphelion cases of ionospheric TEC.

Keywords: TEC, Ionosphere, Diurnal variation, Seasonal variation, Latitudinal variation, Geomagnetic storm Variation, Equatorial Ionization Anomaly, East African low latitude /equatorial region, Fountain effect.

List of Figures

List of Tables

Chapter 1

Introduction

The ionosphere is the upper atmosphere's region with the highest concentration of charged particles. It is created when solar radiation strikes the neutral atoms and molecules of the upper atmosphere where electrons are expelled by the process of photo ionization. The principal source of ionization in the ionosphere are the short wavelength components of solar radiation, that is extreme ultraviolet (EUV) and X-rays which are energetic enough to ionize these atoms and molecules in the Earth's atmosphere [2].

The ionization rate of the ionosphere at various altitudes depends upon the intensity of the solar radiation as a function of wavelength and the ionization efficiency of the neutral atmospheric gases. Since the Sun's radiation is progressively absorbed in passing through the atmosphere, its residual ionizing ability depends upon the length of the atmospheric path and consequently upon the solar zenith angle. The maximum ionization rate occurs when the Sun is overhead but there is a geographic, diurnal and seasonal variations in the ionization rate [3, 4].

When the Sun is directly overhead throughout the day, the intensity of sunlight reaching the upper atmosphere is maximum, and the amount of ionization is largest. On the night side of the Earth, the quantity of sunlight reaching the atmosphere is totally blocked and photo ionization production is at its lowest and recombination is dominant. Photo ionization and recombination mechanisms govern the diurnal fluctuation of the ionosphere in general [5].

Moreover seasonal ionospheric variation is linked to changes in the solar zenith angle. Geomagnetic storms are the outcomes due to the interaction of transferred solar wind energy towards the Earth's magnetosphere through magnetic re connection. They come

into existence as coronal mass ejections (CMEs) from the Sun. CMEs are the primary cause of severe geomagnetic storms. During the geomagnetic storm, the ionosphere is disturbed, which caused the severe changes in TEC [6].

Generally, the plasma density in the ionosphere varies dramatically based on the time of day, altitude, latitude, longitude, season, and geomagnetic activity causing changes in numerous metrics such as the GPS total electron content (TEC). The TEC value, which is produced from the modified GPS signal via free electrons, can be used as an indicator of ionospheric variability. TEC is the total number of electrons in a unit area along the path of a GPS signal from a space satellite to a ground receiver. TEC is measured in units of 10^{16} per square area, where $10^{16} electrons/m^2 = 1$ TEC unit(TECU) [7, 8].

Many researchers have made different studies on GPS TEC over different regions of the world due to the availability of GPS signals under all weather condition on regional as well as global basis which include, TEC variations with diurnal, seasonal, geomagnetic activity and latitudinal variation. According to [9], Bagiya studied in Indian low latitude region the diurnal pattern of TEC exhibits a steady increase from about sunrise to an afternoon maximum and then falls to attain a minimum just before sunrise. And the seasonal variations of TEC shows variation with a peak during the equinox period and a trough during the solstice period. The TEC fluctuation during the geomagnetic storm of August 24, 2005 demonstrates typical low latitude characteristics with the highest value on the storm day and the lowest value on the next day. Response of the total electron content at Brazilian low latitudes to co rotating interaction region and high speed streams (HSS), during solar minimum 2008 by Candido [10]. The result showed that during geomagnetic storms related to HSSs, the ionosphere at low latitudes is highly changeable, with rises and falls in density. The ionospheric electron content can enhance by more than 100 % over the calm day average, especially around the southern peak of the equatorial ionization anomaly (EIA). Observation of Ionosphere Scintillation and Total Electron Content (TEC) Characteristic at Equatorial Region at Malaysia was studied by Ya'acob [8]. The TEC values were quantified in terms obtained from Equatorial GPS measurements. The largest Total Electron Content (TEC) was discovered during noon; the daily peak is usually between 5:00 and 10:00 UTC.

However, in Africa only a few studies were conducted, such as low solar activity variability and IRI 2007 predictability of equatorial Africa GPS TEC [11].

Investigation of TEC variations over the magnetic equatorial and equatorial anomaly regions of the African sector[12] and others were carried out to understand ionospheric variation and irregularities. According to those researchers, the highest daily TEC values were found in the afternoon, while the highest seasonal values were found during equinoctial months, moderate during the summer solstice and least during the winter solstice.

Much as these studies were conducted, still it need further studies to observe the diurnal, seasonal variations of TEC as well as the effects of geomagnetic activities and latitudinal variations on ionospheric TEC within the region. Because of this we are motivated to investigate the ionospheric variability by taking some GPS stations to gain more understanding of the low latitude and equatorial ionosphere in the region of east Africa like Ethiopia (ARMI, ABOO, NEGE, DEBK), in Eritrea (ASAB), in Kenya (MOIU) and in Saudi Arabia (SOLA) GPS receiver stations are selected to study the ionospheric variation in the suitable way, like the diurnal variation, seasonal and geomagnetic behavior is only conducted in Ethiopia, however the latitudinal variation is investigated in Kenya, Ethiopia and Saudi Arabia.

The objective of this study is thus, focused on investigation of the diurnal, seasonal, latitudinal and geomagnetic storm variations of the ionosphere using TEC data taken from the above listed low latitudinal and equatorial ground based GPS receiver stations in the month of March, June and December on selected days based on the Dst index during the year of 2015.

This study is organized by five chapters. Chapter 1 presents introduction including organization of the study, chapter 2 deals about the Earth's atmosphere and ionosphere, atmospheric regions based on temperature profile, ionospheric region and its variability. In chapter 3 GPS with it's working principle it's use for ionospheric TEC are derivations are described. In chapter 4 brief data, methodologies, result and discussions in terms of diurnal, seasonal, geomagnetic and latitudinal variation of TEC are presented. In chapter 5 we presents conclusion and recommendation.

Chapter 2

The Earth's Atmosphere and Ionosphere

2.1 The Earth's atmosphere

The Earth's atmosphere is a thin gaseous envelope that surrounds the planet and extends hundreds of kilometers from its surface, growing thinner (less dense) with distance but always kept in place by Earth's gravitational attraction. The air we breathe is contained in the atmosphere, as are clouds of moisture (water vapor) that form the water we drink. It shields humans from meteorites and dangerous solar radiation while also warming the Earth's surface. In consequence, the atmosphere serves as a protective cocoon for all life on Earth [13]. The neutral atmosphere can be stratified into various sub-levels based on changing temperature gradients.

Troposphere

The troposphere extends from the ground to about 10 km in altitude with a temperature lapse rate of 7 K/km. It ends at the tropopause which is an overlapping region which separates the troposphere from the layer above [14].

Stratosphere

The stratosphere is an area of rising temperature that extends from 10 km to 50 km owing to the ozone layer's absorption of solar UV light, which peaks at approximately 50 km. The termination of the stratosphere is marked by the stratopause.

Mesosphere

The mesosphere is the part of the atmosphere that extends up to around 90 kilometers. Because of radiative cooling, the temperature drops with height here. The mesopause divides the mesosphere from its underlying layer, the thermosphere, where the temperature rises exponentially due to absorption of increasingly energetic portions of solar radiation until it reaches a constant value of around 1000 K at approximately 500 km altitude.

Thermosphere

The thermosphere is an area of rising temperature that extends from 90 km to 500 km. In this case, neutral particles are in diffusive equilibrium, which implies that the vertical distribution of neutrals is regulated by the specie's relative masses (under gravity). The turbo pause is the area approximately 90 km that separates the lower homogeneous atmosphere from the thermosphere. Because of turbulent gas mixing below the turbo pause, the neutral atmosphere is generally homogeneous [15].

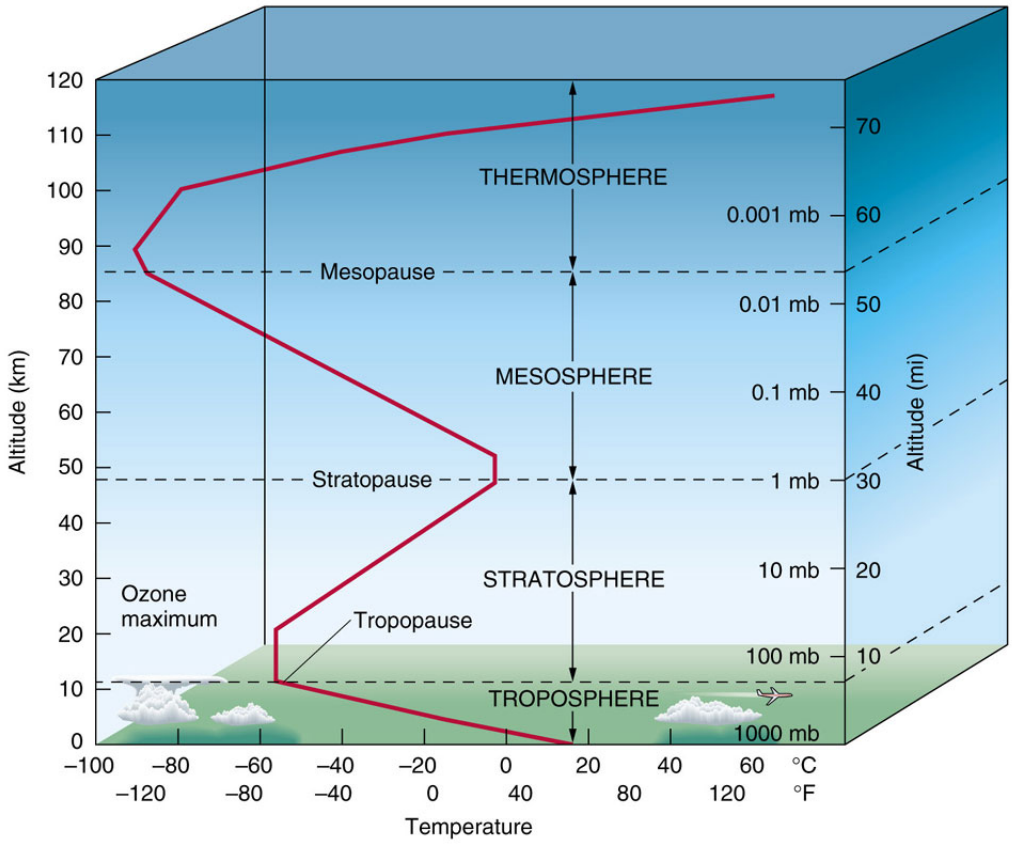

Figure 2.1: Vertical profile of the Earth atmosphere.

2.2 The Ionosphere

The ionosphere is a zone of partly ionized plasma above the Earth's atmosphere that forms as neutral atoms and molecules are photo ionized. A large scale vertical layer of ionization with in the ionosphere is formed by an increase in the density of the atmosphere as we get closer to the Earth's surface, a decrease in the intensity of photons as they bombard neutral atoms and the availability of different atoms and molecules at different heights from the Earth's surface. This causes the ionosphere to exist as a vertically stratified partly ionized plasma state between 60 and 1000 kilometers above the Earth's surface [9, 14].

2.2.1 Ionization and Recombination

Photo ionization is the process by which a photon removes an electron from a neutral atom, resulting in the formation of a positively charged ion. Solar radiations such as extreme ultraviolet (EUV) and X-ray radiations are the primary cause of ionization in the ionosphere. The bulk of electrical activity in the ionosphere is generated by photo ionization (ionization produced by light radiation) (i.e., high-frequency). When an electron from a neutral atom, such as an oxygen atom, collides with an EUV photon, its energy is used to transfer one electron from the neutral atom, enabling it to escape and dart around freely. The neutral atom becomes a positively charged ion after losing a negatively charged electron.

$O + hv\ (\lambda < 91.1nm) \rightarrow O^+ + e^-$

$N_2 + hv\ (\lambda < 79.6nm) \rightarrow N_2^+ + e^-$

$O_2 + hv\ (\lambda < 102.6nm) \rightarrow O_2^+ + e^-$.

The recombination of free electrons with positive ions is a reversal of photo ionization, and the recombination process is the primary driver of neutral atom formation [16]. It is the process by which negatively charged electrons and positively charged ions mix to produce neutral atoms [17].

$O^+ + e^- \rightarrow O + hv$

$O_2 + e^- \rightarrow O + O + hv$

$NO^+ + e^- \rightarrow N + O + hv$

$N_2 + e^- \rightarrow N + N + hv$

2.2.2 Vertical structure of the ionosphere

The plasma density in the ionosphere has a vertical layered structure, indicated by the D, E and F layers due to altitude changes in the atmospheric neutral composition and the production rate with altitude. Each layer is governed by a separate set of physical processes and has its own set of primary ions. Typically, the F layer is split into two layers. The lowest layer is called the F_1, here the ionization is produced through the photo ionization process and disappears through recombination processes with the electrons. The next sub layer where the transition from chemical to diffusion occurs is called the F_2 layer. Here the maximum electron density usually occurs [18].

D region

The D region, which spans 60 to 95 kilometers is the ionosphere's lowest point. It is a weakly ionized plasma area with concentrations on the order of $10^6/m^3$ that usually vanishes at night. Ionization sources include very energetic charged particles, like the galactic cosmic radiation (GCR) and the most energetic part of solar radiation which is in the X-ray spectrum range with wavelengths less than 10 nm and energies in the order of 100 keV, EUV radiation less than about 110 nm and hydrogen Lyman α emission line (121.6 nm) ionizing nitric oxide (NO).

E region

Ionization of atomic and molecular oxygen contributes to the formation of E region by high energetic X-ray radiation and Lyman β radiation (102.6) nm. The predominant ions are O_2+, $NO+$ and the typical plasma density is in the order 10^{11} per meter cubic. Solar X-ray (0.8 - 14 nm) and UV radiation (79.6 - 102.7 nm) ionize the neutral particles to form the E region.

F region

F region is produced mainly by radiation in the range of 14 - 79.6 nm. On the day side, the F region is split into two sub layers, F1 and F2 depending on its major constituents. It extends from about 150 km to more than 500 km above the surface of Earth. It is the less dense layer of the ionosphere, which implies signals penetrating this layer will escape into space. At higher altitudes the number of oxygen ions decreases and

lighter ions such as hydrogen and helium become dominant. This layer is the topside ionosphere. Extreme ultraviolet (10 - 100 nm) solar radiation ionizes atomic oxygen. The F layer consists of one layer at night, but during the day, there are F1 and F2 layers [14].

Table 2.1: Characteristics of Different Ionospheric Layers

Layer	Major ion	Basis of formation(principal photo ionization)
D	NO^+, O_2^+, N_2^+	L_y α 121.6nm ionizes NO, X-rays 0.1-1nm, cosmic ray
E	O_2^+, NO^+	L_y β 102.6nm, EUV 91.1-102.7nm, Ionizes O_2, x-ray 1-17 nm
F_1	O^+, NO^+	HeII 30.4nm , EUV 17-91.1nm ionizes O
F_2	O^+	HeII, UV and upward diffusion from the F_1 layer

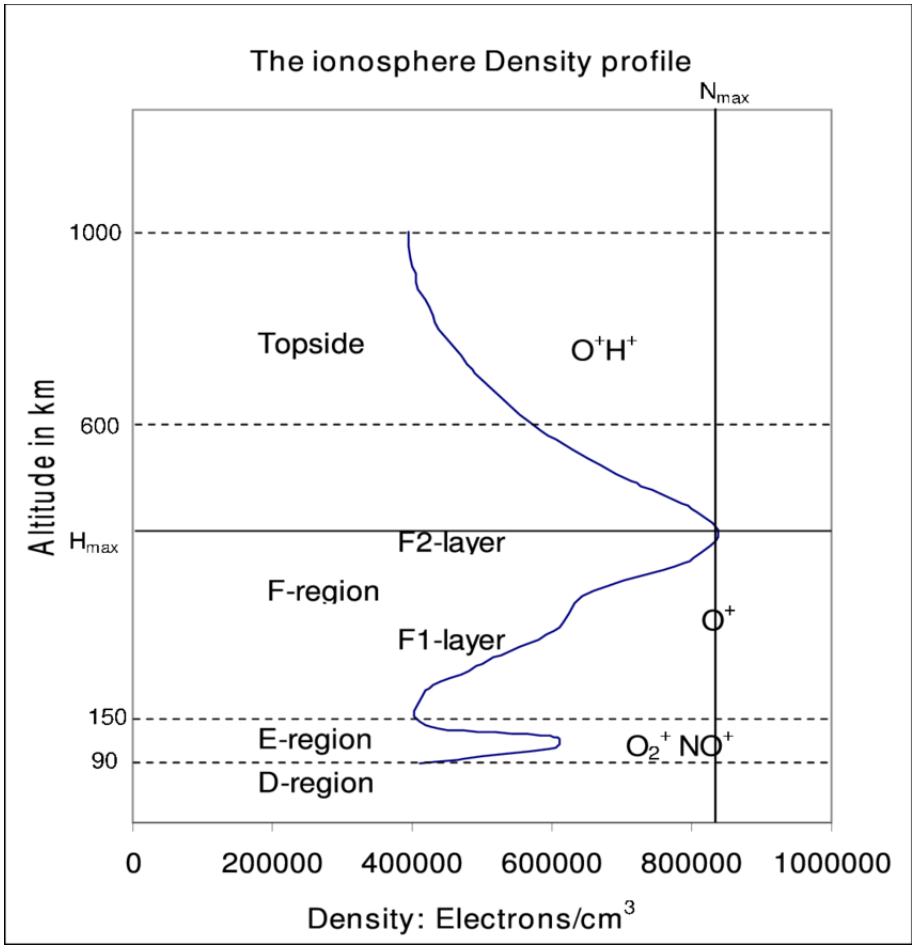

Figure 2.2: The different layers of the ionosphere and their predominant ions are displayed at their particular heights.

2.3 Ionospheric Variations

The ionosphere varies in different ways because the principal source of ionization, solar UV and X-ray intensity varies with the position of the sun at a given location on the planet. As a result, the ionosphere's electron density fluctuates in response to solar activity.

2.3.1 Diurnal Variations

The ionosphere's electron density varies from day to night. Because recombination rates are higher at night in the absence of ionization. At noon the daytime electron density reaches its highest point. Since, the ionosphere has a diurnal fluctuation during the day and night. The intensity of solar radiation rises as the Earth spins in relation to the Sun, and ionization likewise increases peaking at midday. Maximum frequencies steadily fall during the night reaching their lowest soon before sunrise [19, 20].

2.3.2 Seasonal variations

In the northern hemisphere, the seasons are grouped into three categories which are the vernal and autumn equinox, summer solstice and winter solstice. The months for summer in the northern hemisphere indicate winter in the southern hemisphere, and vice versa. But only maintaining the equinox months as it is for the northern hemisphere. During equinox the Sun shines directly on the equator and the length of day and night is nearly equal. Because of this there is maximum photoionization [20, 21]. At different time of year the sun is vertically above different geographic locations. At equinox noon (March 21, September 23) the sun is vertically above observer at the equator and vertically above observer at the Tropics of Capricorn and Cancer or solstice dates (21 December and 21 June). As vertical illumination from the sun results in higher ionization rates, higher electron density concentration are observed at these locations on these dates than at other locations [22].

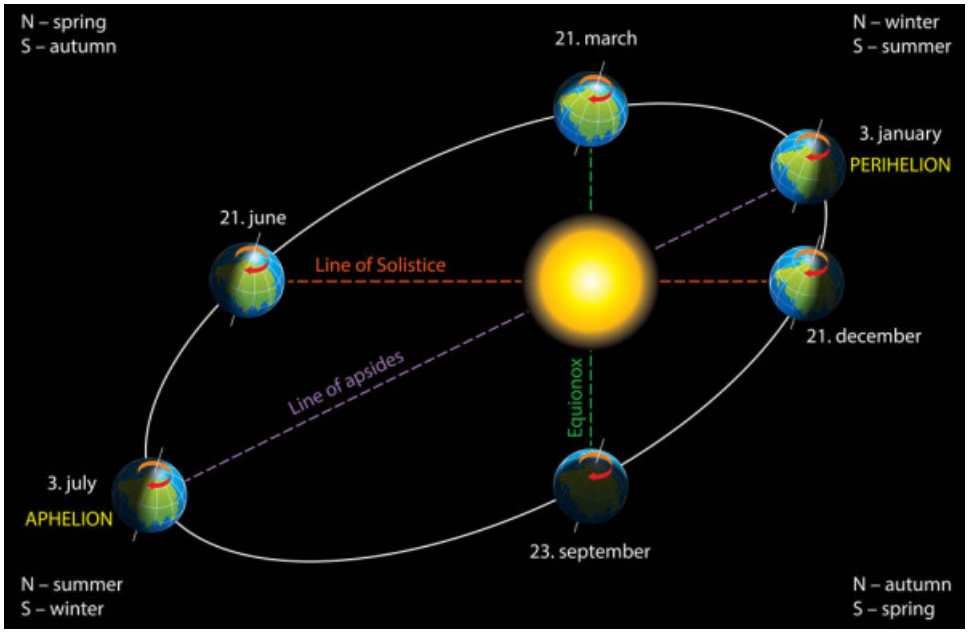

Figure 2.3: Earth's position relative to the Sun

2.3.3 Latitudinal variations

With increasing latitude, the intensity of radiation and the production of free electrons reduce. The geomagnetic field is horizontal at the geomagnetic equator, and the electric field is eastward during the day and westward at night owing to air motion [19].

2.3.4 Geomagnetic storm variation

The geomagnetic storm is a severe global disturbance of the Earth's magnetic field, usually under the impact of disturbances in the solar wind and interplanetary magnetic field (IMF) with their origins near the solar surface. Extensive studies have shown that intense geomagnetic storms are usually caused by coronal mass ejections (CMEs) [23]. Throughout the 11-year solar cycle regions of instability in the sun can release high speed plasma containing large amounts of matter and energy known as coronal mass ejections (CMEs). These solar CMEs eventually infiltrate the earth's magnetosphere and create significant disruptions in the earth's magnetic field taking about 20 hours to travel from the sun to Earth [24, 25].

Geomagnetic storms result in an increase of the ring current, and the magnetic field generated by the ring current is superimposed on the geomagnetic field, which causes great changes in the horizontal component H. When a geomagnetic storm occurs, Earth's entire magnetic field will be continuously disturbed for several hours to tens of hours, and all geomagnetic elements will undergo drastic changes. A high-speed solar wind stream (HSS) is another solar wind disruption that offers favorable circumstances for geomagnetic storms. HSSs plow through the slower solar wind in front of them, forming co rotating interaction regions (CIR). These areas are frequently associated with geomagnetic storms, which, while less powerful than CME storms may deposit more energy in the Earth's magnetosphere over a longer period of time [26].

An early phase, a major phase and a recovery phase are the three phases of a geomagnetic storm, respectively. A substantial depression of the magnetic field on the Earth's surface is the distinguishing feature of the main phase of a geomagnetic storm. The result is a strongly southward driven interplanetary magnetic field (IMF-Bz), which intensifies energy input in the upper atmosphere and energizes the ring current. The strength of the low latitude magnetic disturbance storm time index (Dst), which is a measure of the intensity of the magnetospheric ring current is generally used to

identify a geomagnetic storm [27]. Depending on the Dst index, geomagnetic storms are classified as weak storm (Dst =-30 nT to -50 nT), moderate storm (Dst = -50 nT to -100 nT), intense storm (Dst = -100 nT to -200 nT) and severe storm (Dst less than -200 nT) [28].

2.4 Geographic Regions of the Ionosphere

There are three major regions of the global ionosphere. These are the low latitude region , mid latitude and high latitude regions.

2.4.1 Low latitude Region

The ionosphere of the Earth in the equatorial (low latitude) zone is markedly different from that of the mid and high latitudes. This is because the equatorial ionization anomaly (EIA), which is characterized by an electron density trough region at the geomagnetic equator and a dual band of enhanced electron density (crest regions) around ±15 north and south of the trough, dominates the low latitude ionospheric F area [12]. The diurnal change of the zonal electric field, which generally points eastward during the day and reverses at night, forms the EIA. The ionospheric plasma is lifted upward by vertical $\vec{E} \times \vec{B}$ drift at equatorial latitudes in conjunction with the horizontal northward geomagnetic field. Due to gravitational and pressure gradient pressures, plasma diffuses downward along geomagnetic field lines into both hemispheres once it has been transported to higher altitudes [21, 29].

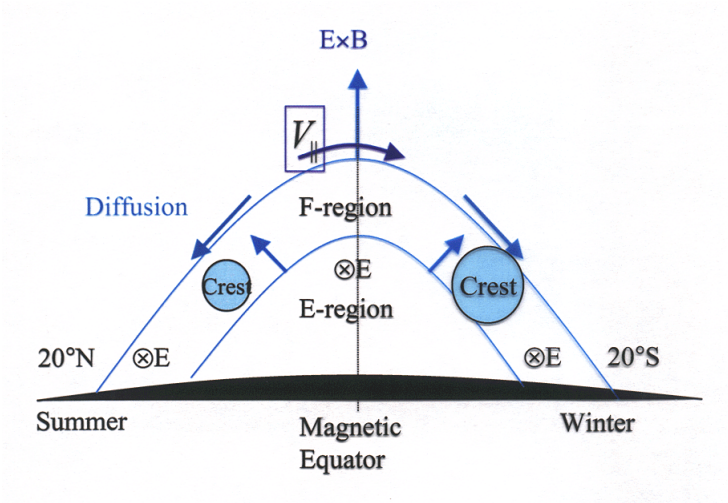

Figure 2.4: Fountain effects and asymmetry of the equatorial anomaly.

2.4.2 Middle Latitude Region

The ionosphere at mid-latitude is also the least disturbed and changeable of all the zones, acting as a buffer between high-latitude activities and low latitude phenomena [30].

2.4.3 High Latitude Region

The auroral and polar cap areas of the high latitude ionosphere are separated by the ionospheric trough, which is located on the equator ward side of the auroral zone. The structure of the Earth's geomagnetic field is responsible for divides in this area. In the ionosphere photoionization by ultraviolet and x-ray light is not the only source of ionization. Ionization of neutral gases by energetic particle impact plays a major function at high latitudes.

Energetic particles produced by the Sun are confined within the Earth's magnetic field and move along magnetic field lines to the high latitude ionosphere [4].

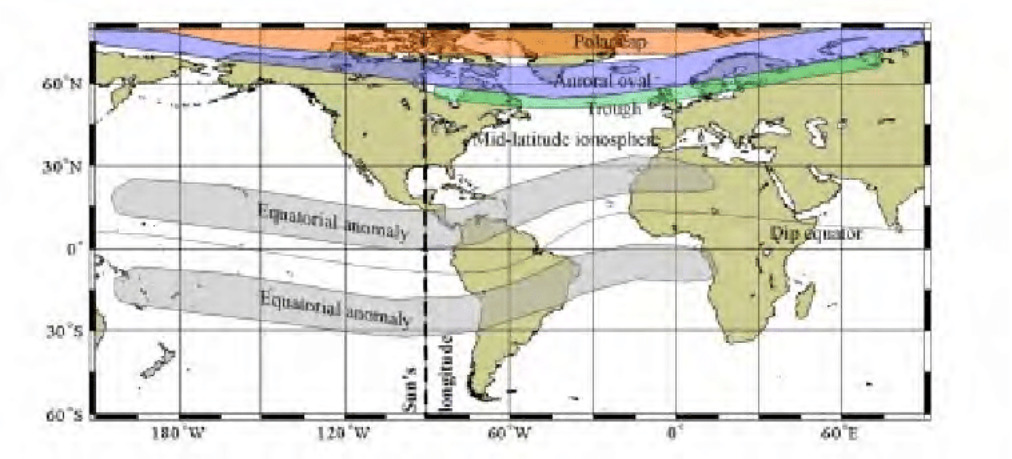

Figure 2.5: Geographical regions of ionosphere

Chapter 3

The Global Positioning System

The Global Positioning System (GPS) is a satellite based navigation system that uses distance measurements from satellites to determine precise and immediate location and time. The GPS system provides users with proper equipment with precise, continuous, three-dimensional location and velocity information from across the world.

It is a working system that provides users all over the globe with exact three dimensional position and time that is traceable to global time standards 24 hours a day, 7 days a week [31]. GPS works by sending radio waves L1=1575.42 MHz and L2=1227.60 MHz from satellites to ground receivers, airplanes and other satellites. Due to the total amount of free electrons along the course of the signals from the satellite to the receiver, the carrier experiences a phase advance and the code experiences a group delay when GPS signals pass through the ionosphere [32].

3.1 GPS segments

According to its organizational structure, the GPS system can be divided into three segments: the space segment, the user segment and the control segment.

The space segment

It consists of 24 satellites circling the Earth at 20,200 Km in altitude. The signals can cover a larger region because of the high altitude. The satellites are arranged in their orbits so, a GPS receiver on Earth can always receive a signal from at least four satellites at any given time. Each satellite sends out low-power radio signals with a unique code on several frequencies, which the GPS receiver can detect. The primary purpose of these coded signals is to calculate the time it takes for a signal to travel from a satellite to a GPS receiver. The travel time multiplied by the speed of light equals the distance from the satellite to the GPS receiver [33].

The control segment

The control segment comprises a ground based network of master control, data uploading and monitor stations. In the case of GPS two master control stations(MCS) one primary and one backup four data uploading stations and ten monitor stations located throughout the world. The satellites are tracked by the control section, which then provides them with adjusted orbital and temporal data. Four unmanned control stations and one master control station make up the control segment. The four unmanned stations collect data from the satellites and transfer it to the master control station, which corrects it before sending it back to the GPS satellites [34].

The user segment

The user segment consists of equipment that processes the received signals from the GPS satellites and uses them to derive and apply location and time information. The equipment ranges from handheld receivers used by hikers, to sophisticated, specialized receivers used for high-end survey and mapping applications [34, 35].

3.2 GPS Observables (measurement)

GPS measurements can be derived using two fundamental observations: pseudo range and carrier phase. The GPS receiver generates a replica of the two L band frequencies transmitted by the satellites and receiver differences it with the incoming doppler shifted signal to produce a beat frequency. The signals transmitted by the satellites and received at a GPS user's receiver form the GPS observable, which are manipulated to attain position estimates. The principles of GPS navigation formulations containing different types of GPS measurements are guided by those observable [36].

3.2.1 Code Pseudo ranges

The pseudo range is a measure of the distance between the satellite and receiver's antenna. The distance is measured by measuring the GPS signal transmission time from the satellite to the GPS receiver's antenna. This refers to the distance between the satellite at the time of GPS signal emission and the GPS antenna at the time of GPS signal reception. The transmission time is measured through maximum correlation analysis of the receiver code and the GPS signal. The receiver code is derived from the clock used in the GPS receiver [32].

3.2.2 Carrier Phases

The GPS carrier phase is defined as the difference between the received doppler shifted carrier signal and the constant receiver generated reference frequency. It is a measure of received phase signal of a satellite relative to the receiver generated carrier phase at the reception duration. The received signal phase is tracked by shifting the receiver generated phase [21, 36].

3.3 GPS Error Sources

GPS signals propagates along their fixed paths from the satellites to the receiver stations by crossing with different mediums as a result the GPS may be exposed to different errors. These errors classified as those originating from the satellites, those coming from the receiver and the others are due to signal propagation medium [1, 37].

3.3.1 Satellite based errors

The ephemeris error, satellite clock error, relativistic effects owing to various gravitational potentials encountered by satellites and the satellite instrumental bias error are all mistakes that originate from the satellite.

Ephemeris error

When the GPS message fails to send the correct orbital parameters ephemeris problems occur. The ephemeris parameters are transmitted to users as part of the navigation message after being uploaded to satellites. A small residual error exists due to difference between the actual satellite position and the position predicted by the MCS. The ephemeris error can be eliminated by establishing a network of reference stations that broadcast the three-dimensional error in the reported ephemeris or the projected ephemeris based on the reference station's own observations.

Relativistic effects

The general and special theories of relativity have an impact on the satellite clock. The satellite clock would run faster than the reception clock, according to the general theory of relativity, due to the difference in gravitational potential experienced by the satellite and receiver clocks. According to the special theory of relativity a clock aboard the satellite traveling at a constant speed would appear to operate slowly in comparison to a clock on the ground .

3.3.2 Receiver based errors

Multi path error, receiver clock error, measurement noise and instrumental bias error are all faults that originate in the receiver.

Receiver clock error

GPS receivers utilize crystal clocks that are less precise than satellite clocks because they are less costly. As a result, the receiver clock error is significantly larger than the satellite clock error.

Multi path error

Due to reflections from the Earth and objects in the area of a receiving antenna, the signal arrives to the receiver through numerous pathways. The reflected signals are overlaid on the desired direct-path signal, causing the direct path signal's amplitude and phase to be distorted. Both code and carrier phase measurements are affected by multi path, although the amount of the inaccuracy differs substantially.

Receiver measurement noise

Random measurement noise, which includes thermal noise produced by the antenna, amplifiers, cables and receiver multi access noise caused by interference from other GPS like signals and signal quantization noise affects GPS measurements.

Receiver instrumental bias

The frequency dependent transmission delays induced by the analog circuitry within the receiver cause an instrumental bias error. Dual frequency receivers have an instrumental bias error that is unique to them. The ionospheric delay measurements are also affected by the receiver inter frequency bias or differential instrumental bias.

3.3.3 Errors due to Propagation medium

The delay of the GPS signal as it passes through the ionospheric and tropospheric layers of the atmosphere is one of the signal propagation errors.

Ionospheric delay

The presence of free electrons in the ionosphere alters the velocity (speed and direction) of the GPS signal as it travels from the satellite to the receiver. The ionosphere has an impact on GPS signal transmission by delaying code phase measurements and speeding up carrier phase observations [34].

Tropospheric delay

The existence of neutral atoms and molecules in the troposphere has an impact on GPS signals. Both the code phase and carrier phase measurements are delayed due to the troposphere. At GPS frequencies, the troposphere is non dispersive, unlike the ionosphere [1, 37].

3.4 Total Electron Content on the Ionosphere

Total electron Content (TEC) is a frequently used ionospheric measure that is defined as the number of electrons in a column with a cross sectional area of one meter squared that spans between the receiver and the satellite. It is a measure of ionospheric variability obtained from free electrons in a modified GPS signal. Its observations have been extensively utilized to investigate the ionosphere's overall architecture and variability under both geomagnetically calm (periods without ionospheric disturbance) and disturbed circumstances (space weather events) [38, 39].

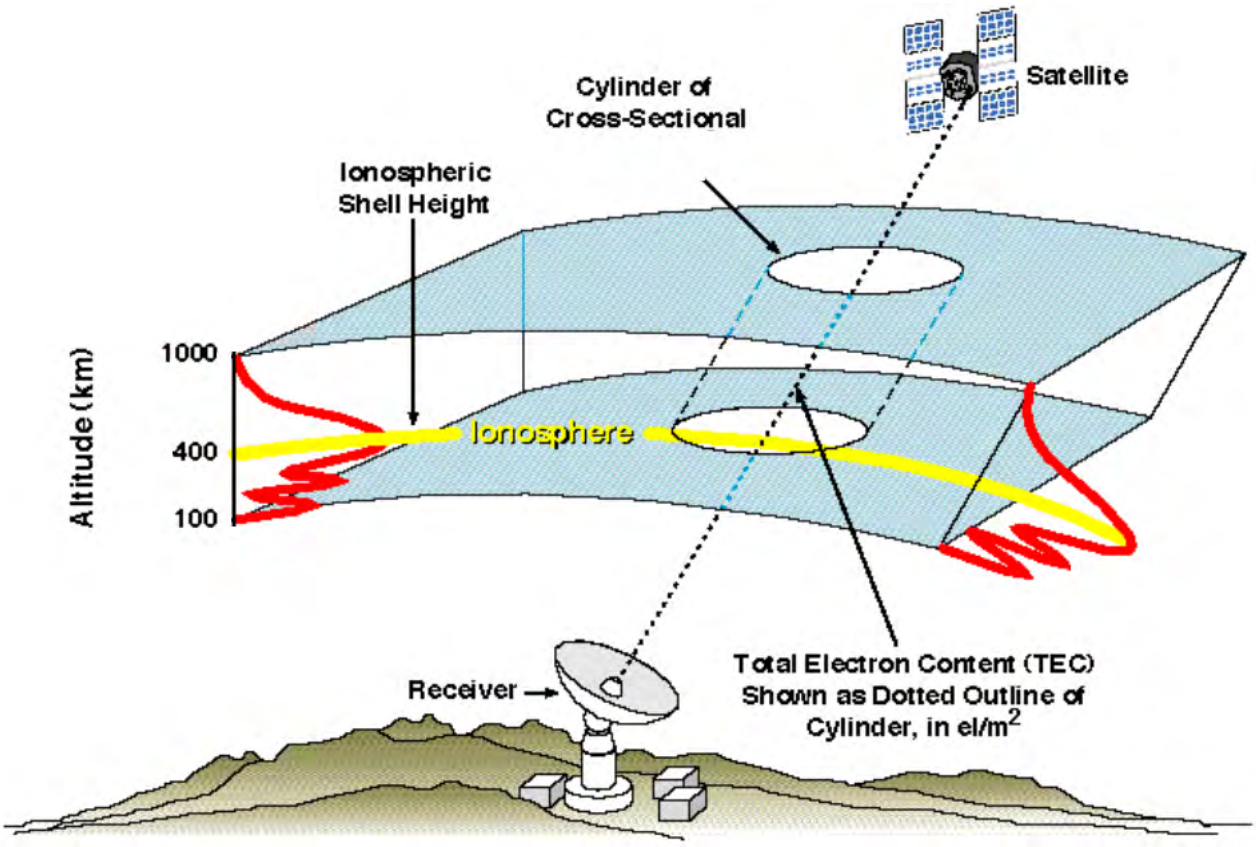

Figure 3.1: Concept of Total Electron Content (TEC) demonstration [1]

3.4.1 Estimation of Ionospheric TEC using dual frequency GPS signals

One of the most significant methods for studying the Earth's ionosphere is to use dual frequency GPS receivers to obtain TEC values. TEC is an ionospheric variability indicator obtained from a modified GPS signal transmitted via a free electron filled medium. It also has the most significant impact on GPS signals. TEC is defined as the total number of electrons present within a cross section 1 m^2 along the integrated path from the satellite to the receiver to each GPS, this is known as Slant Total Electron Content(STEC) [40]. It can be expressed in total electron content units (TECUs) as follows:

$$TEC = \int_{receiver}^{satelite} N_e \, ds$$

, where N_e is the electron density [9, 29]. GPS receivers provide both L carrier phase delays and pseudo P ranges of dual frequencies.

The relative phase delay between the two carrier frequencies can be calculated using two different methods. The first pseudo distance approach produces an absolute TEC scale with less precision, while the second differential phase method improves measurement accuracy.

The TEC inferred from the pseudo range measurement is given by;

$$TEC_p = \frac{1}{40.3}\left(\frac{f_1^2 f_2^2}{f_1^2 - f_2^2}\right)(p_2 - p_1)$$

where, p_1 and p_2 are pseudo range observables on L1 and L2 signals.

Similarly, the TEC from carrier phase measurement can be given as;

$$TEC_\phi = \frac{1}{40.3}\left(\frac{f_1^2 f_2^2}{f_1^2 - f_2^2}\right)(\phi_1 - \phi_2)$$

where, $\phi_1 - \phi_2$ is equivalent to $L_1\lambda_1 - L_2\lambda_2$ the two carrier frequencies f_1 and f_2 are coherently derived from the fundamental 10.23 MHz frequency f_0.

$f_1 = 154 f_o = 1575.42$ MHz, where $\lambda_1 = \frac{c}{f_1} \approx 190$mm $f_2 = 120 f_o = 1227.60$ MHz, where $\lambda_2 = \frac{c}{f_2} \approx 244$mm, λ_1 and λ_2 are wavelengths corresponding to f_1 and f_2 and c is the speed of light in a vacuum (3×10^8 $\frac{m}{s}$).

3.4.2 Single Layer Ionosphere

Using the ionospheric mapping function, the slant TEC value along the path can be converted into the VTEC at the Ionospheric Pierce Point(IPP) based on the single layer shell model hypothesis [40, 41]. All free electrons in the ionosphere are supposed to be concentrated in a single layer thin shell at the height of the major electron concentration in the ionosphere, and the ionosphere can be thought of as a thin single layer enclosing the Earth at a fixed height from the Earth.

In terms of zenith angle χ at the ionospheric piercing point (IPP) and zenith angle θ at the receiver position on the ground, the relation ship between STEC and VTEC can be given by;

$$VTEC = STEC\,(\cos\theta) \text{ where, } \theta = \arcsin\left[\frac{R_e}{R_e+h_m}\sin\chi\right]$$

$$VTEC = STEC\left\{\cos\left[\arcsin\left(\frac{R_e}{R_e+h_m}\sin(\chi)\right)\right]\right\}$$

R_e, is the mean Earth's radius in Km, h_m is the ionospheric effective height above the Earth's surface which is the height of maximum electron density at the F2 peak, which is commonly taken to be 350 km, θ is the zenith angle at the receiver position on the ground and χ is zenith angle at the ionospheric piercing point (IPP) [42].

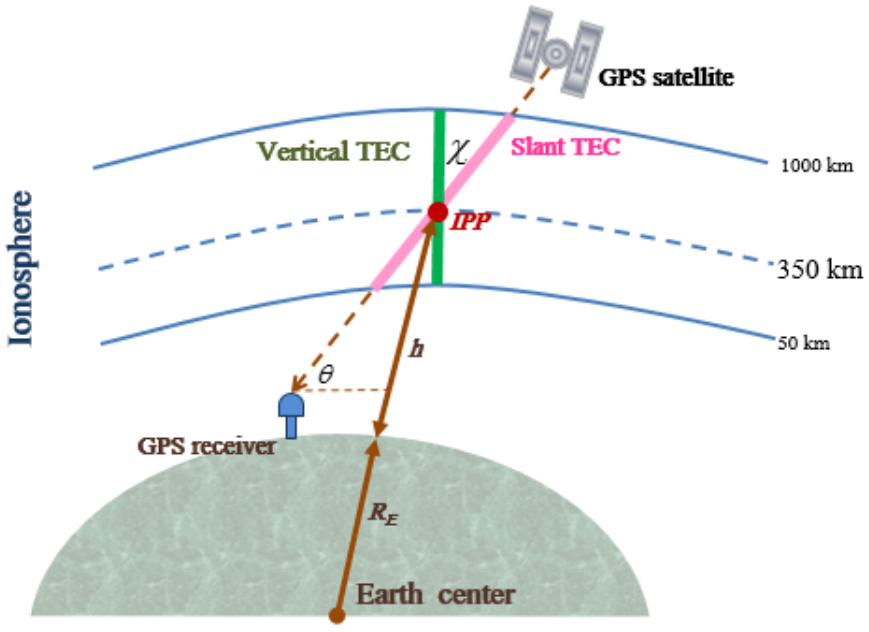

Figure 3.2: The conversion of slant TEC to vertical TEC

Chapter 4

Data Source, Methodology and Discussion

4.1 Data And Methodology

The observational data used in this study were obtained from University NAVSTAR Consortium (UNAVCO) home page: (https://www.unavco.org/data/gps-gnss/gps-gnss.html), which were the VTEC measured at every 15 sec interval from the GPS receivers in receiver independent exchange format (REINEX) data. The data was taken in 2015 on the selected days of equinox month of March, the summer solstice month of June and the winter solstice month of December based on Dst index for the GPS receiver stations of East African region at Arbaminch, Ambo, Assab and Debark to study the diurnal, seasonal and space weather event behavior of TEC, and for study the latitudinal variation the data were taken from stations in Kenya (moiu), Ethiopia (nege, aboo and debk) and one in Saud Arabia (sola) GPS stations. The Dst index data was obtained from the geomagnetic equatorial Dst index home page (http://wdc.kugi.kyoto-u.ac.jp/dstdir/). This GPS TEC data were processed by the GPS TEC application software developed at Boston College by Gopi Seemala software taken from: (https://seemala.blogspot.com/2020/12/gps-tec-program-version-3-for-rinex-3.html) [43].

The TEC analysis software uses the phase and code values for both L1 and L2 GPS frequencies to eliminate the effect of clock errors and tropospheric delay to calculate relative values of slant TEC. In order to avoid the multi path effects, different authors have used observation data above certain cutoff mask ranging from 15° to 35° [44]. In

this study, an elevation cutoff mask of 20° was used for all VTEC computed. This data was scaled down to plot hourly values in terms of VTEC(TECU) versus Universal time(UT) at all stations using the Matlab program software.

Table 4.1: Geographic and Geomagnetic regions of the GPS receiver stations

stations	station code	Geog.latitude	Geographic.longitude	Geomagnetic.latitude
Kenya	moiu	$0.005°N$	$35.3°E$	-2.63°S
Borena negele	nege	$5.3°N$	$39.58°E$	$1.59°N$
Arbaminch	armi	$6.1°N$	$37.6°E$	$2.65°N$
Ambo	aboo	$8.99°N$	$37.8°E$	$5.45°N$
Assab	asab	$13.1°N$	$42.6°E$	$8.75°N$
Debark	debk	$13.15°N$	$37.9°E$	$9.52°N$
Saud Arebia	Sola	$24.9°N$	$46.4°E$	$19.8°N$

4.2 Discussion and Analysis

Make use of the GPS TEC data obtained from the GPS receiver stations (refer Table 4.1) we have studied the diurnal and seasonal variation using the data taken from Armi, Aboo, Asab and Debk and for geomagnetic storm day Ambo is chosen for this study. Because it's TEC value shows the effect of geomagnetic storm on TEC rather than other GPS stations and for latitudinal variations of ionospheric TEC in Ethiopia (Ambo, Borena negele, Debark), in Kenya (Moiu) and in Saudi Arabia (Sola) GPS stations show latitudinal dependence of TEC. In the following sub section, we will show these variations.

4.2.1 Diurnal Variation of Ionospheric TEC

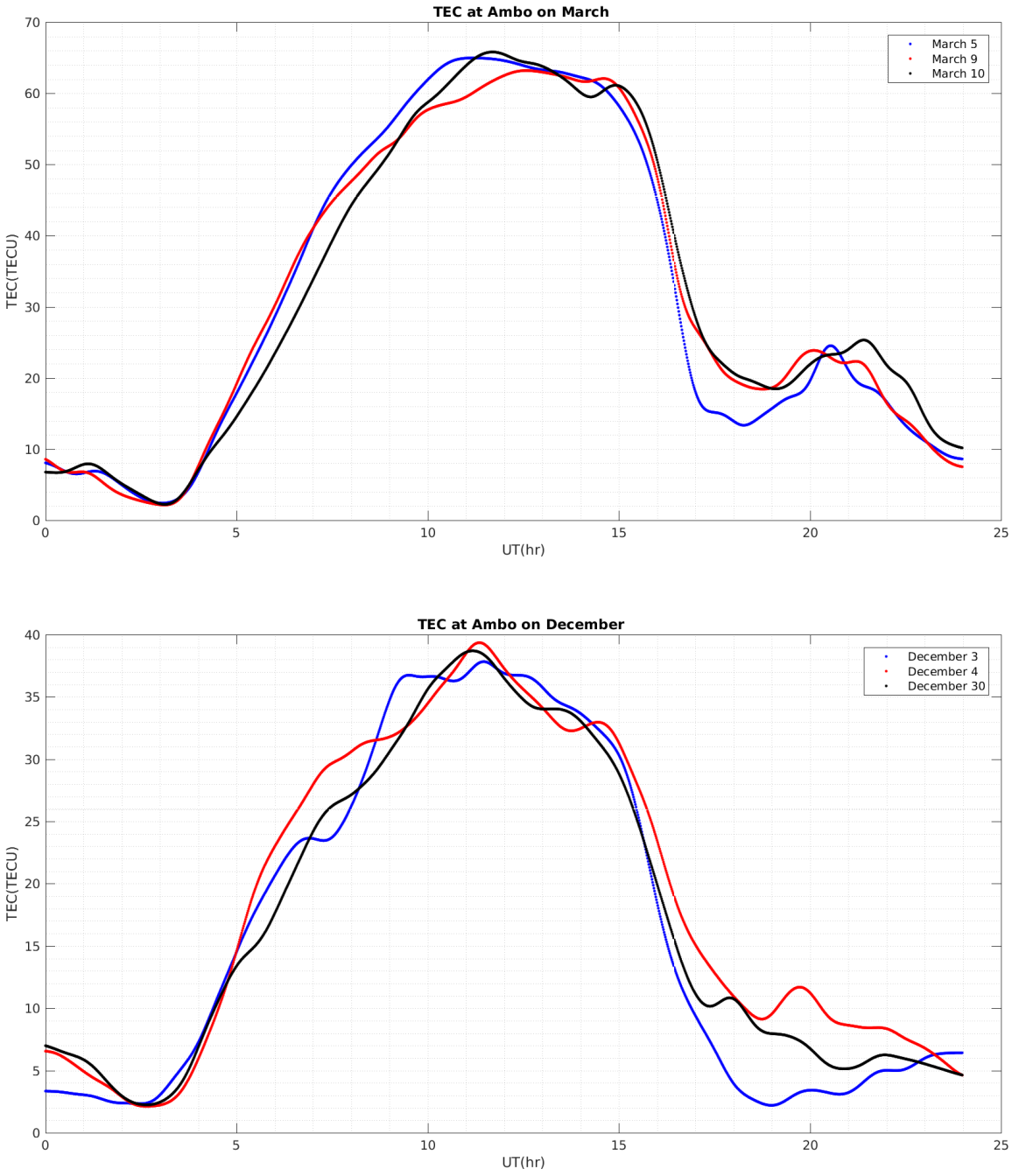

Figure 4.1: Diurnal variation of TEC observed at ABOO GPS receiver station in March and December, 2015

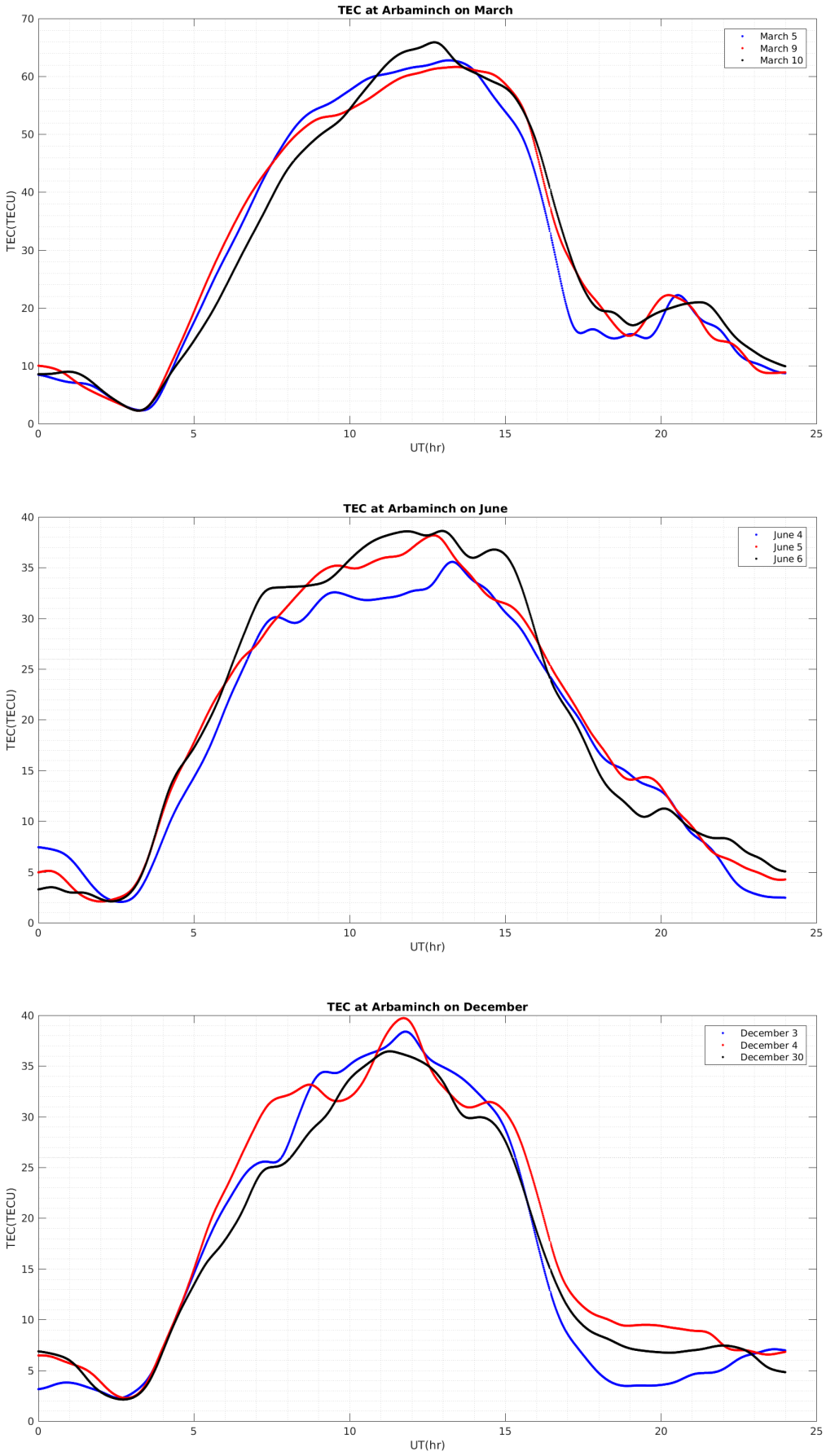

Figure 4.2: (Diurnal variation of TEC observed at ARMI GPS receiver station in March, June and December, 2015)

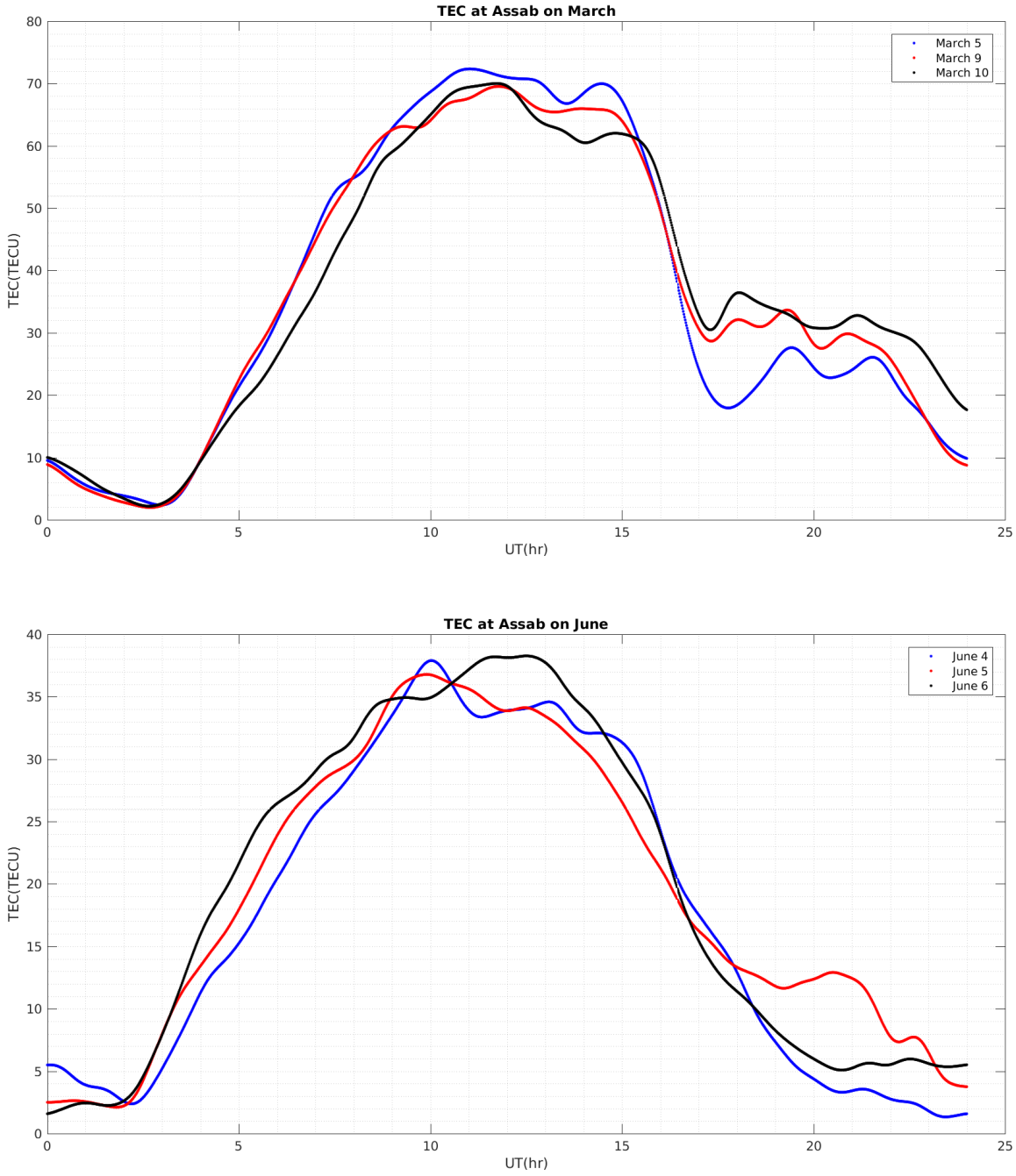

Figure 4.3: Diurnal variation of TEC observed at ASAB GPS receiver station in March and June, 2015

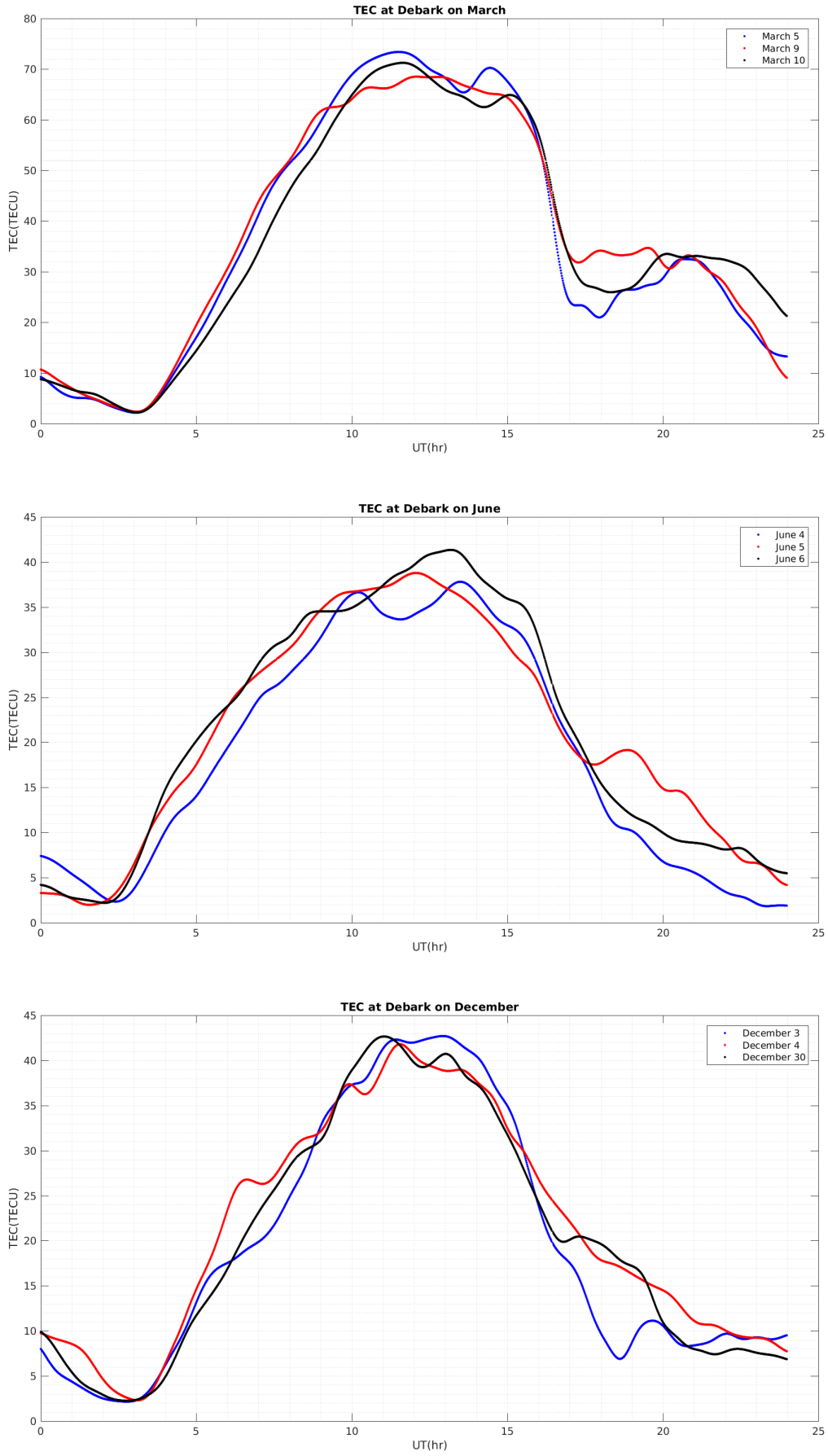

Figure 4.4: The Diurnal variation of TEC observed at DEBK GPS receiver station in March, June and December, 2015

From Figure 4.1 the TEC value for ABOO shows steadily increase and a plateau region between 10:30 UT and 15:00 UT. The peak TEC measured on March 10 afternoon around 11:39 UT which is 65.8 TECU. However in the morning and evening the amount of TEC is almost similar and it is less than the peak value. Similarly in December the TEC value shows increase during the day time with the maximum peak value is about 39.33 TECU around 11:25 UT.

In Figure 4.2 for ARMI Peak value of TEC 65.86 TECU was observed in March in the afternoon around 12:46 UT. However, on June exhibited TEC maximum peak value is about 51.02 TECU at 13:24 UT, while on December the maximum TEC value is around 39.7 TECU at 11:46 UT.

In Figure 4.3 for ASAB Peak value of TEC 72.1 TECU were observed on March, in afternoon around 11:39 UT. On the other hand, in June the TEC maxium peak value is about 35.28 TECU around 11:33 UT while, on December the maximum TEC value is 37.4 TECU around 11:50 UT.

In Figure 4.4 for DEBK Peak value of TEC 73.55 TECU were observed on March, at afternoon around 11:37 UT. However, on June 20 the TEC maximum peak value is about 40.2 TECU around 14:13 UT while on December 4 the maximum TEC value is 42.39 TECU around 13:34 UT.

As one can see in all the above plots (Figure 4.1 up to Figure 4.4), the TEC value shows two types of variations. The first one is the hourly variation, which may be attributed to the small change in activity of the Sun itself. This means that the sunspot number and different particles (solar wind) coming from the Sun are different from day to day and hour to hour. The second one is the large scale dawn-dusk/day-night variations in the TEC value. The TEC value falls continuously during night and attains a short lived minimum at dawn. Then starting from sun rise, the TEC value began to rise during the day till it attains a maximum occurring around noon, when Sun is overhead. This rise in TEC value shows that there is photo ionization of the atmosphere due to increased intensity of the solar radiation during day starting from sunrise. The TEC value then began to decrease during night starting from sunset at 15:00 UT to 23:00 UT. This decrease of the TEC value during night shows that the intensity of solar radiation of sun has decreased and thus there is no further ionization of the atmosphere and the reverse recombination process dominates during night. Therefore, the photo ionization follows sun's direction (zenith angle) as the Earth rotates about

its axis and as a result the day and night time electron density of the ionosphere is not the same [22, 45]. The diurnal fluctuation of TEC generally shows that an increase from around dawn to an afternoon maximum, then drops to a minimum just before sunrise. The diurnal variation of TEC in Ethiopia (Ambo, Arbaminch and Debark) and Eritrea (Assab) shows many characteristics typical to low latitude ionosphere such as a vertical total electron content (VTEC) minimum at predawn and gradual increase with the time of the day attaining a maximum in the afternoon and a gradual decrease after sunset. Large variations of TEC are observed in day time while night time variations are found to be almost constant. The variations of the diurnal TEC can be divided into three different sections. These are: the build up region, the day time plateaus and the decay region. This is the result of change of the production and loss rates of electrons in the ionosphere [12, 46]. The extensive ionization that occurs as the sun rises increases the electron concentration around the F2-peak at a rate that is essentially determined by the rate of production. Because TEC is proportional to the ionospheric plasma's maximum electron density. During the day, as the temperature rises, the production rate rises as well, eventually surpassing the loss rate. As a result, the TEC gradually rises from a morning minimum to an afternoon maximum value. Late in the afternoon, when the temperature drops, the loss rate rises and overtakes the production rate. The TEC values gradually fall as a result of this. Because the principal source of ionization is no longer present in the evening, TEC values stay low. Moreover, the TEC value shows a wider plateau region in equinox month of March than the solstice months of June and December. This may be due to the fact that in March the northern and southern hemisphere are equally heated and a large portion of the Atmosphere is exposed to solar radiation, the maximum solar radiation is received during the whole day and the TEC value doesn't fall till sunset. Then the slope of TEC value versus UT graph (rate of decrease of TEC) is higher than for equinoctial month of March the solstice months. This is because the TEC value is high which implies that there is more electron density in the atmosphere and thus the electron lose rate due recombination is proportional to the square of the electron density and due to attachment is proportional to the electron density [47]. For the solstice month of December, the TEC value rise steadily reaches maximum and then began to fall slowly with no plateau region showing more TEC value fluctuation in afternoon. This may be due to the existence of the high sun spot number during in December than in

March. In addition to this, the equinox month of March shows a secondary minimum-maximum during night at about 21 UT. The equatorial electrojet (EEJ) during day and the counter electrojet (CEJ) during night are enhanced in this month. Therefore, the secondary minima maxima during night may be attributable to the CEJ.

4.2.2 Seasonal Variation of Ionospheric TEC

The seasonal variation of ionospheric TEC over the four GPS receiver stations that is, Arbaminch, Ambo, Assab and Debark, in selected days of the year, 2015 are shown in the following figures. The plots in Figures 4.5 and 4.6, clearly show that the seasonal variations of ionospheric TEC at the four stations for the three seasons in the selected days of March, June and December. As we can seen from the figures the ionospheric TEC value attains a maximum on the equinoctial month of March and the TEC value in the winter solstice month of December is minimum while the TEC value in the summer solstice month of June has an intermediate value. It may be the result of the position of the Sun relative to the equator that affects the ionization process in the ionosphere because the intensity of the ionizing radiation depends on the solar zenith angle. That is, when the sun is at different positions the solar zenith angle is also different so that the rate of ion production would be different.

During the equinoctial months, the sun is overhead at the equator, and the temperature in this area is warmer than at the pole. As a result, the equatorial meridional wind blows from the equator to the poles. Due to the increased effect of wind transport during high solar activity, the neutral composition changes and the O/N_2 ratio increases at equatorial and low latitude locations. Because an increase in the O/N_2ratio results in a higher electron density, the equatorial ionization anomaly is expected to be more developed at the equinoxes than at the solstices [9].

When the Sun is at horizon the intensity of the solar radiation reaching the equatorial ionosphere is relatively small compared to the intensity reaching at the equatorial ionosphere from the overhead Sun. This is the result of the fact that the Earth does not move at a constant speed in its elliptical orbit, therefore, the seasons are not equal length and as a result the amount of solar radiation received is different. The relative position of the Earth's axis to the Sun changes during the cycle of seasons. During the solstice the Sun is not overhead at the equator, that means the light intensity that pass through the ionosphere above the equator is small compared to the equinox which leads to small value of TEC in the ionosphere [48].

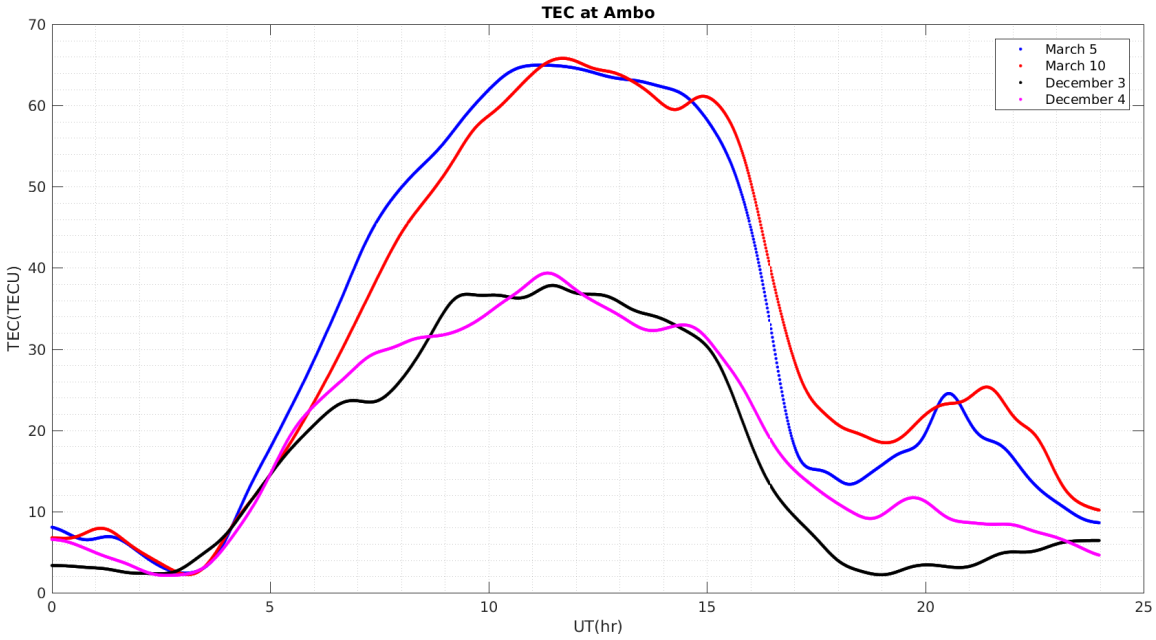

(a) The variation of TEC value for selected March equinox and December solstice days at ABOO

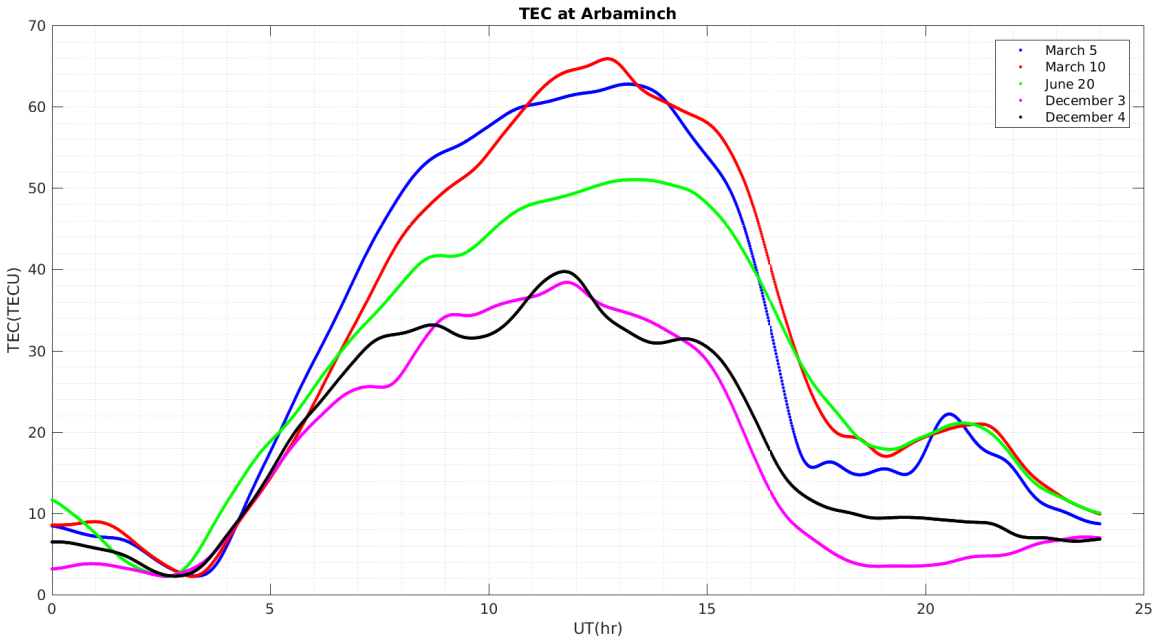

(b) The variation of TEC value for selected March equinox, June and December solstice days at AR

Figure 4.5: Seasonal variation of TEC at Ambo and Arbaminch GPS receiver stations

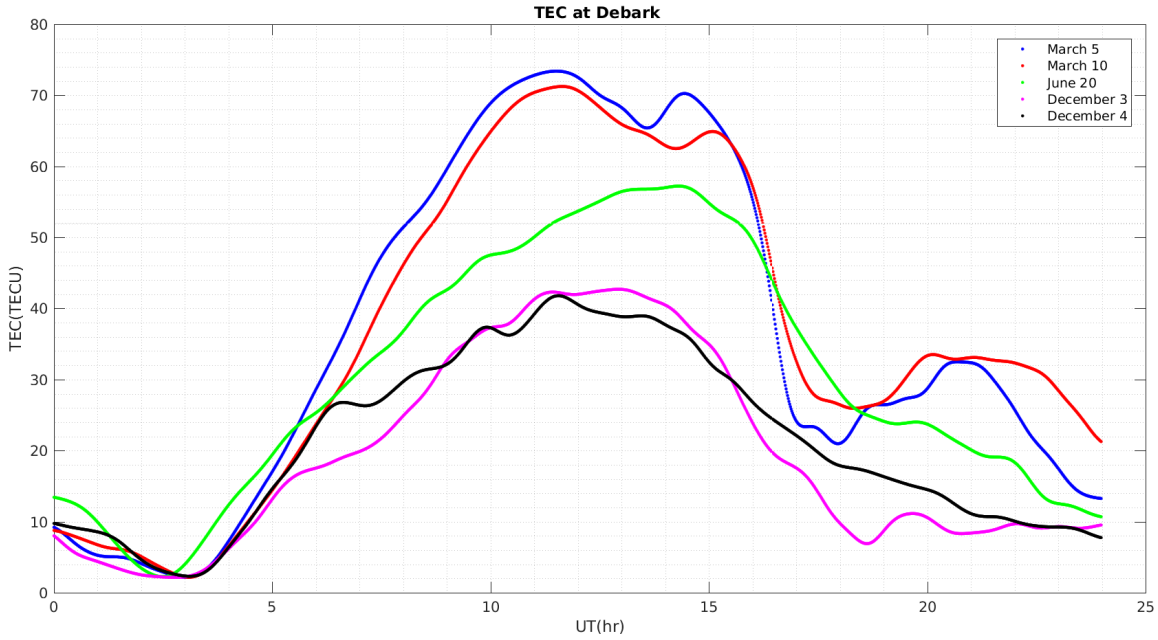

(a) The variation of TEC value for selected March equinox, June and December solstice days at DE

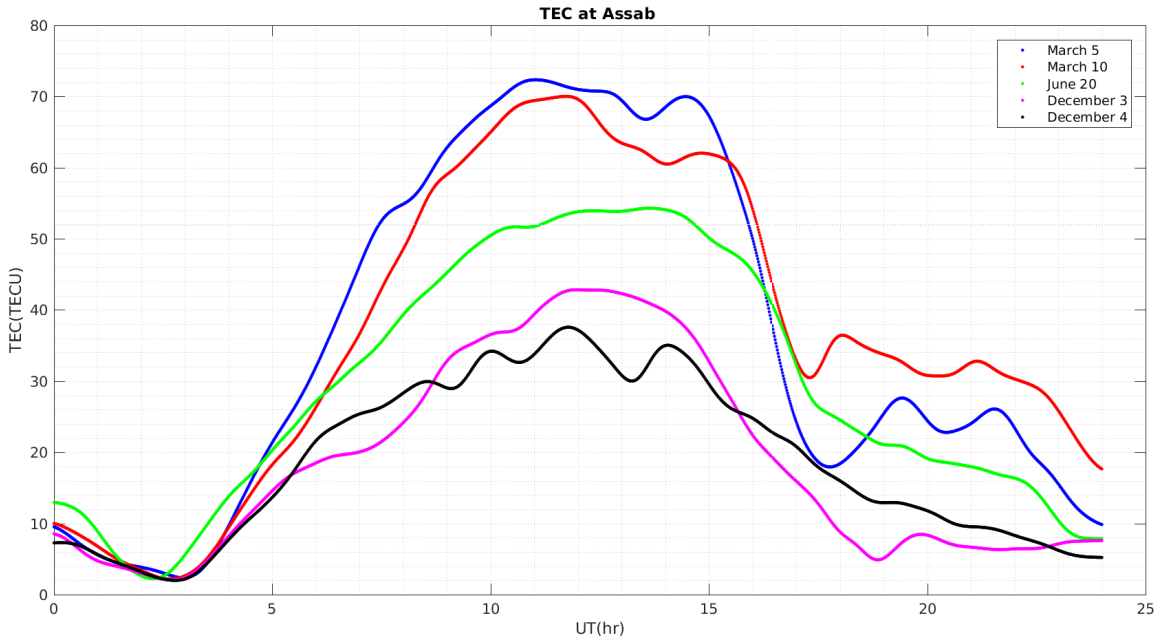

(b) The variation of TEC value for selected March equinox, June and December solstice days at AS

Figure 4.6: Seasonal variations of TEC at Assab and Debark GPS receiver stations

In general, the TEC value in the equinox month of March is greater than the values in the solstice months of June and December because of the positions of the sun. In the June solstice month, the sun is in the northern hemisphere and the axis of the Earth is inclined towards the sun and thus the solar zenith angle is small. This increases the

intensity of the solar radiation so as to give rise to more photo ionization. Moreover, in June the day is longer and receives more radiation during the longest day which in turn gives rise to more photo ionization. On the other hand, in the December solstice the day is short and the axis of the Earth is inclined away from the Sun which results in less radiation and thus less photo ionization. Because of these reasons, the TEC value in June is greater than that in December.

In this study the highest TEC value were observed in the equinoctial month, moderate in the summer solstice, and then least in the winter solstice, exhibiting the seasonal variation. our result is consistent with [49] utilizing GPS SCINDA data from an equatorial anomaly station in Uganda to study TEC fluctuation. They found that TEC values were highest during the equinoctial months, moderate throughout the summer, and lowest during the winter solstices. The other researcher [50] the diurnal variation of the ionospheric time delay was studied in an Indian equatorial anomaly location, with the diurnal variation being greatest during the equinoctial months and least during the winter solstices. Therefore, our results appear to correspond with the conclusions of this investigation.

4.2.3 Variation of Ionospheric TEC with Earth Distance from the Sun

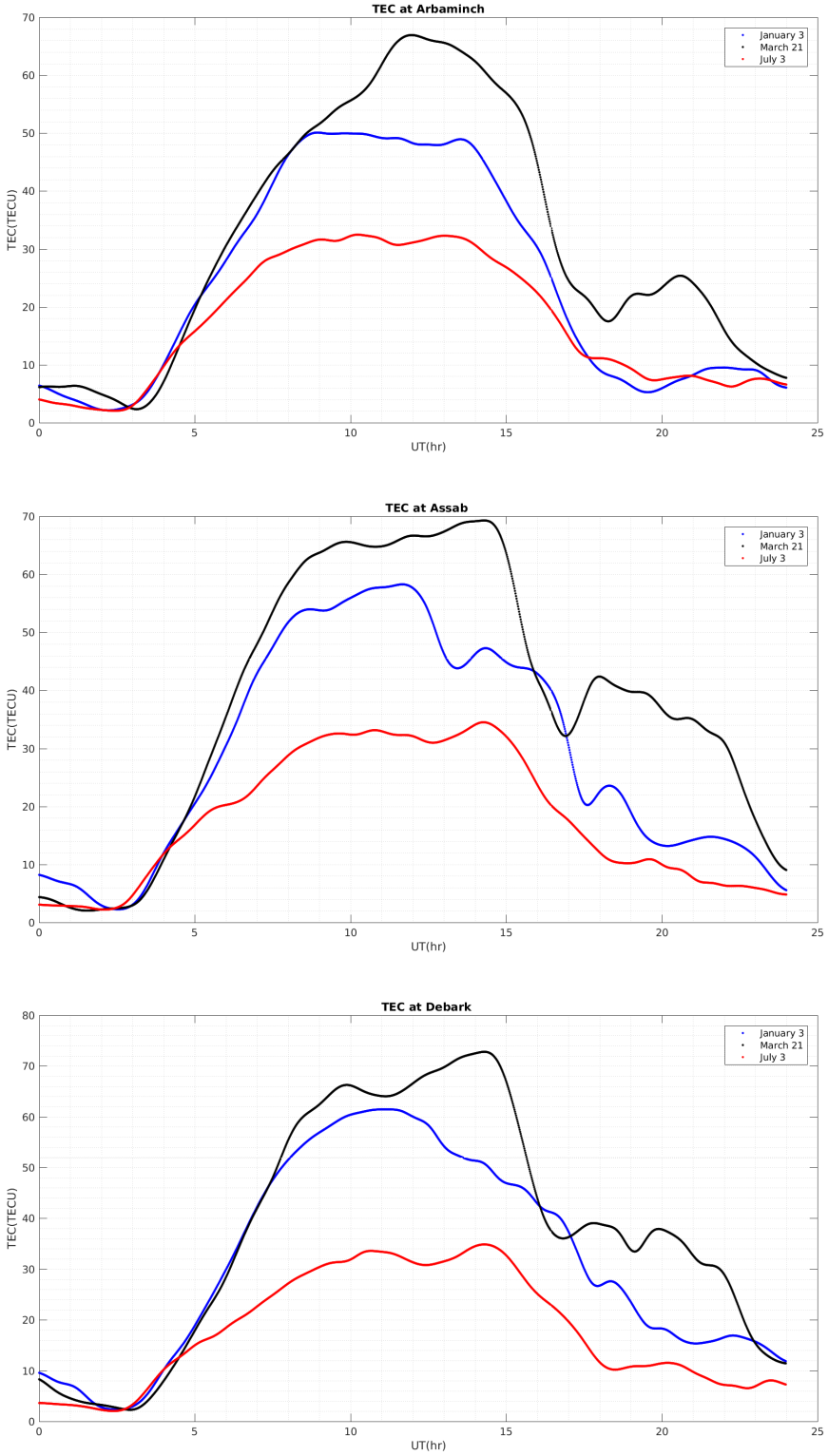

Figure 4.7: Variations of TEC at ARMI, ASAB and DEBK over head (March 21, 2015), at perihelion (January 3, 2015) and at aphelion (July 3, 2015)

Figure 4.7 shows the variation of TEC at the Earth at the aphelion (the Earth far from the Sun's position) and perihelion (the Earth closer to the Sun's position). From the figure we see that the TEC value in the aphelion is less than the TEC value in the perihelion position of the Earth. This is may be because the solar activities of the sun in January 2015 is greater than that in July. Since the activity of the sun increases the ionization of the atmosphere which increases the TEC value. In addition to this on January 3, the Earth is very close to the Sun (at perihelion position) and the Southern hemisphere is relatively closer and the zenith angle is smaller where as the northern hemisphere is relatively farther and the solar zenith angle is larger. Because of this the southern hemisphere is more heated as it receives intense solar radiation on January 3 and its atmosphere becomes more ionized. This differential heating of the two hemisphere give rise to meridional winds that blow from southern hemisphere to northern hemisphere and thereby drags the ions from south to north. On the other hand, on July 3 the the Earth is at it's farthest distance from the Sun. The northern hemisphere is relatively closer to the sun and it is inclined towards the sun and thus receives more ionizing solar radiation than the southern hemisphere. But because of the enhanced differential heating of the atmosphere, the initiated meridional wind carries the ions from the northern hemisphere to the southern. This may be cause for the annual asymmetry of TEC value, where the January 3 TEC value is greater than that of the July 3. However, the TEC value of the winter Solistic month of December is less than that of the Summer solistic month of June, which is the seasonal anomaly. There may be other factors to explain the annual asymmetry of the January 3 and July 3 TEC value. More or less we have assumed those assumptions, but it requires other investigation with regard to to the annual asymmetry of the the two selected days of the January 3 and July 3.

4.2.4 Variations of Ionospheric TEC during geomagnetic storm

One most intense geomagnetic storm has occurred on March 17, 2015. The begining of the main phase of March 17 was 0700 UT, 2015 with minimum Dst index of -223 nT during the main phase of the geomagnetic storm and the Dst values measured on this day shows intense geomagnetic storm. During this phase, the interplanetary electric field penetrates the ionosphere at low latitudes for several hours and transferring energy from the solar wind to the magnetosphere. This causes interplanetary particles to be loaded into the magnetosphere-ionosphere area, then increasing the ring current in the terrestrial environment [51]. As followed by this the depression of the magnetic field during the main phase is explained as the effect of the ring current in the magnetosphere. The ring current is largely transported by energetic ions with energies ranging from 20 to 200 keV. As the number of energetic particles increases, the ring current to east increases. Generally, the nature of the main phase of a geomagnetic storm provides an explanation of the process of the ring current energization responsible for the development of the storm. The geomagnetic storm under examination on March 17 has a maximum Dst index depression of more than 100 nT, which indicates a high ring current intensification and a shock wave that has reduced the Earth's magnetic field. When solar wind energy is deposited in the magnetospheric polar cap area, however, the geomagnetic field is disrupted. As a result of this disruption, energy inputs from the magnetosphere to the upper atmosphere can cause a considerable shift in electron density in the F area of the ionosphere.

Solar wind energetic particles can enter the magnetosphere along magnetic field lines, resulting in plasma injection on the magneto sphere's night side or they can become stuck on closed geomagnetic field lines, generating radiation belts in the terrestrial environment. Due to the magnetic field gradient the confined particles show drifts. Because drifts are determined by charge sign, ions go west and electrons east, resulting in a ring current. The ring current generates a surface magnetic field that is diametrically opposed to the Earth's magnetic field and is inversely proportional to the ring current's energy content, which rises during geomag netic storms [52].

In this study to investigate the effects of the geomagnetic storm on TEC, the GPS TEC data obtained from ABOO station is shown in Figure 4.9. To see the effects of storm on TEC, seven days were considered, one day before storm day, during the storm day, four days after a storm day and one day the quietest day of the month of March.

Before the storm day which is the initial phase of a storm day there is no fluctuation of ionospheric parameter even if on March 16 it is the initial phase of the geomagnetic storm. As one can see in the figure during the main phase of the storm on March 17 the ionospheric TEC is enhanced with its fluctuation around 1500 UT, in this phase energy is transferred from solar wind to the magnetosphere. This produces loading of the interplanetary particles in to the magnetosphere ionosphere region and enhances the ring current with in the terrestrial environment [12]. This produces a strong decline of Dst index during the storm's main phase and enhancement of ionospheric TEC value. At the recovery phase of the storm on March 18 after 1100 UT this phase is associated with the loss of the ring current particles from the magnetosphere. During this phase the magnetic field on the Earth's surface goes back to the value of quiet time like the quietest day of March 10, because of the decay of the ring current.

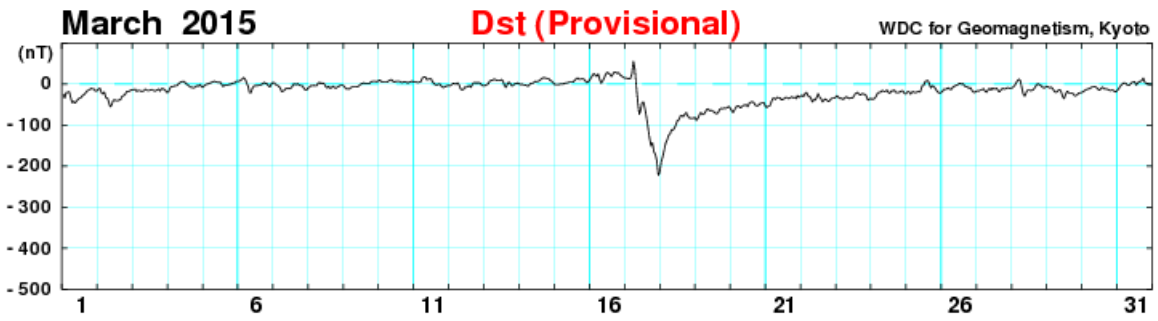

Figure 4.8: WDC for Geomagnetism, Kyoto hourly equatorial Dst Values in March, 2015

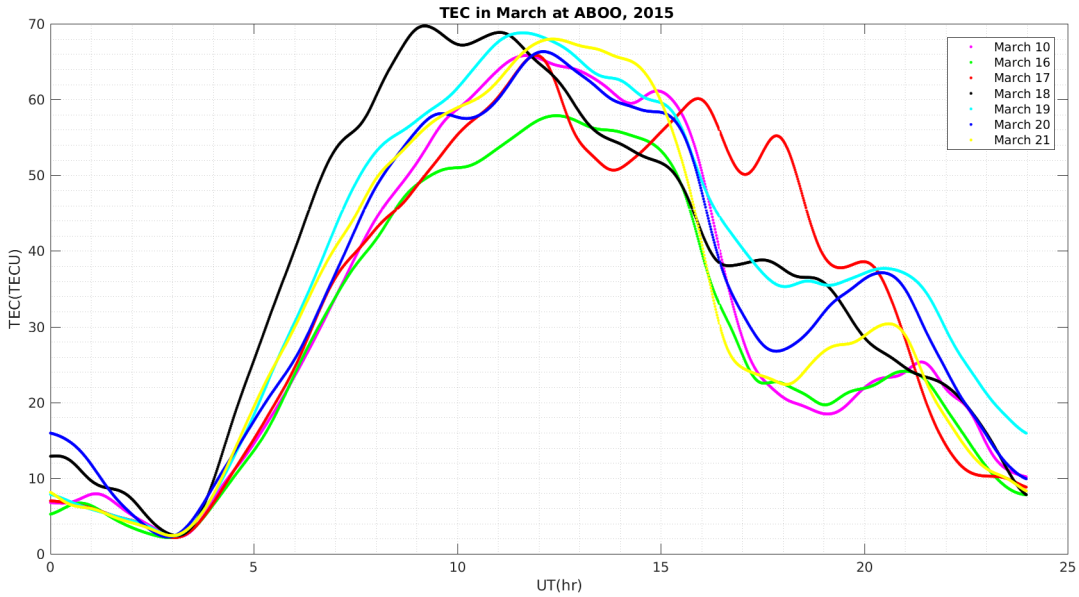

Figure 4.9: TEC at Ambo on March quiet day, initial, main and recovery phase, 2015

4.2.5 Latitudinal Variations of TEC

One of the basic dynamic properties of the equatorial and low latitude ionosphere is the Equatorial Ionization Anomaly (EIA), which is a unique structure consisting of two ionization peaks on each side of the geomagnetic equator at around 15° geomagnetic latitude, with a trough in ionization between them.

Table 4.2: Geographic and Geomagnetic regions of the stations

stations	Station code	Geographic.latitude	Geographic.longitude	Geom.latitude	
Kenya	moiu	$0.005°N$	$35.3°E$	-2.63°S	
Borena negele	nege	$5.3°N$	$39.58°E$	$1.59°N$	
Ambo	aboo	$8.99°N$	$37.8°E$	$5.45°N$	
Debark	debk	$13.15°N$	$37.9°E$	$9.52°N$	
Saud Arebia	Sola	$24.9°N$	$46.4°E$	$19.8°N$	

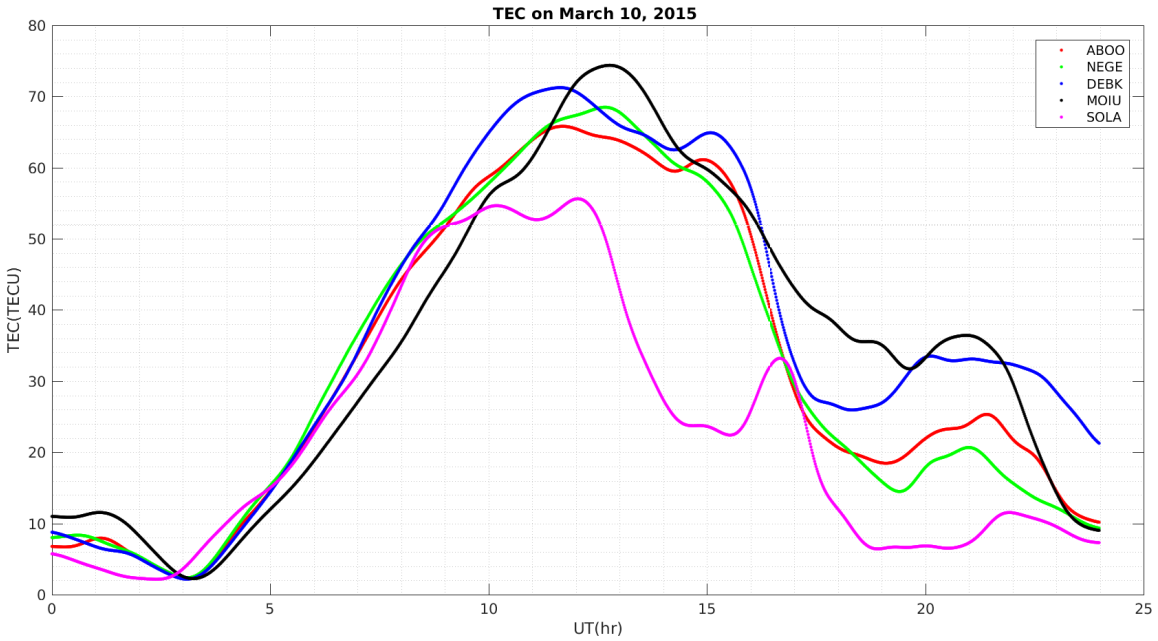

(a) The variation of TEC on March 10 at 5 GPS receive stations

Figure 4.10: Latitudinal variations of TEC at different GPS receiver stations.

As one can see in Figure 4.10 there is a latitudinal difference between the list of different GPS receiver stations (refer Table 4.2). Due to this latitudinal variation, the five GPS receiver stations show different value of TEC. The largest peak value of TEC occurs for MOIU station which is closer to geomagnetic equator and hence inside the trough of EIA region. This increase may be due to the enhanced equatorial fountain effect as on March 10, the sun slightly in the southern hemisphere almost overhead on MOIU. This high TEC value happens as the high solar radiation intensity near the equator results in higher ionization that generates high electron density, which forms the equatorial plasma [45]. This plasma is lifted vertically upward to higher altitude by the $\vec{E} \times \vec{B}$ vertical drift force and then the electrons began to diffuse along the magnetic field lines to higher latitudes due to the forces of gravity and pressure gradient. At this high altitude the atmospheric density is very low so that electron loss due recombination and attachment is a very slow process and thus the electron lives for a longer time in the upper ionosphere (F2 layer), which may increase the TEC value. Equatorial ionization anomaly occurs in regions close to the equatorial anomaly [12]. Negele is closer to geomagnetic equator than MOIU but its TEC value is less than that of MOIU. This is because the Sun is in the southern hemisphere on March 10, almost overhead to MOIU than to Negele and thus MOIU receives more radiation than NEGE and thus more ionization. The next peak value of TEC is observed at DEBK station. This increase may be because Debark is closer to Northern crest of EIA region, where there is a high electron density. The least value of TEC peak value is observed at the station of SOLA located beyond the equatorial anomaly region, where TEC value decreases. Therefore, in this study the ionization peaks at the station will thus depend on the time of maximum electric fields which drive currents, the time taken for vertical drifts and the diffusion time for electrons once lifted [11, 53]. If diffusion time is less the electron lives for a longer time overhead of the station and thus it's TEC value is higher, even if it is located in the trough of EIA rgion.

In addition to the day time variation of TEC, the nighttime enhancements of TEC (secondary maxima) were observed over MOIU, NEGE, ABOO and DEBK stations and the highest enhancements in TEC occur at the SOLA station where SOLA is at a slightly higher latitude north of EIA crest. The TEC value of SOLA decreases quickly just after noon time as it is far from the geomagnetic equator where atmospheric ionization is enhanced. Just after suset, its TEC value rises to mini secondary maxima

that is short lived. The occurrence of secondary maxima of the night time TEC peak of SOLA may be the consequence of the northward diffusion of the excess electron density in the crest region. Then Debark's secondary TEC peak appears which at slightly lower latitude north of EIA crest. The occurrence of secondary maxima of the night time TEC peaks of DEBK must be the consequence of two factors. The first one is the south ward diffusion of the excess electron density in the crest region of EIA. The second factor is due to northward diffusion of the early lifted ionospheric plasma near geomagnetic equator during daytime. Because of these two factors the night time TEC peak of DEBARK exhibits a plateau region for longer night time while the others decrease quickly. Moreover, the night time minima of NEGE is less than that of AMBO while the day time TEC peak of NEGE is higher than that of ABOO. This strange night time behavior may be due to the fact that NEGE is closer to the geomagnetic equator and thus the plasma that is lifted to higher altitude may diffuse northward and southward to higher latitudes and as a result ABOO may receive these electrons and its night TEC is higher than that of NEGE [46, 54].

In addition to this the secondary night time maxima of the stations closer to the geomagnetic equator may be due to the Counter Electrojet (CEJ). This TEC enhancement of the station close to the geomagnetic equator arises from increased westward electric fields just after sunset which causes the CEJ [12].

Chapter 5

Conclusion and Recommendation

5.1 Conclusion

The diurnal, seasonal, geomagnetic storm and latitudinal dependency of TEC was investigated in this work. Owing to the strength of solar radiation, the diurnal pattern of TEC ranges from a predawn low to a maximum during the afternoon, and subsequently declines throughout the night due to the presence of recombination and the absence of ionization.

The seasonal variation result shows that the highest TEC values are typically recorded during equinox season of March, whereas the lowest peak values are found during the December solstice and intermediate value is found in the summer solstice of June. The TEC value in March shows a very rapid decrease after sunset due to the high recombination rate that is proportional to the square of the high electron density in March. Moreover, the night time TEC value shows a secondary mini maxima near dawn which may be due to the Counter Electrojet (CEJ). The TEC value in the solstice months of June and December don't show plateau and secondary maxima. It simply increase till noon and then decreases slowly during afternoon and during night.

The geomagnetic storm dependency of TEC shows the TEC value on the geomagnetic storm day is greater than that on the quite day. Moreover, the fountain effect that causes the equatorial ionization anomaly (EIA), which is enhanced during the storm time. In addition to these, the latitudinal variation of ionospheric TEC was also investigated. The TEC profiles also vary with latitude. The highest TEC value is obtained for stations that are closer to the geomagnetic equator (MOIU in Kenya) and the least TEC value is obtained for stations that far from the geomagnetic equator

(SOLA). DEBK which is around the northern crest of EIA, the NEGE and ABOO have intermediate value which are found in the EIA region and SOLA station recorded the least of TEC value due to farthest from the EIA region and doesn't get the high amount of the radiation value. The TEC value of January 3, 2015 (at Perihelion) is greater than that of the July 3, 2015 (Aphelion), where both are less than the March 21, 2015.

5.2 Recommendation

In order to investigate ionospheric TEC variation, this study did not cover all East African GPS receiver stations. Future research should include all GPS receiver stations in East African countries, as well as many elements that influence the ionospheric TEC value, such as the number of sun spots, radiation flux, and equatorial ionization anomaly, atmospheric gravity wave and tides. Furthermore, many researchers, like researchers on the ionosphere do not think that the aphelion and perihelion cases of July 3 and January 3, which are the Earth's farthest and closest periods relative to the sun, have an effect on ionospheric total electron content (TEC), which is not a seasonal variation but rather an annual asymmetry. In account of this, I hope that in the future, academics would try to examine and identify the basis behind this though.

Bibliography

[1] A. Komjathy, *Global ionospheric total electron content mapping using the Global Positioning System*. PhD thesis, University of New Brunswick Fredericton, 1997.

[2] M. Jones, M. Codrescu, and J. Gannon, "A statistical comparison of vertical total electron content (tec) from three ionospheric models," in *AGU Fall Meeting Abstracts*, vol. 2008, pp. SA51A–1554, 2008.

[3] R. Bureau, "Handbook—the ionosphere and its effects on radiowave propagation," *International Telecommunication Union: Geneva, Switzerland*, 1998.

[4] J. A. Bittencourt, *Fundamentals of plasma physics*. Springer Science & Business Media, 2004.

[5] A. W. Wernik, L. Alfonsi, and M. Materassi, "Ionospheric irregularities, scintillation and its effect on systems," *Acta geophysica polonica*, vol. 52, no. 2, pp. 237–249, 2004.

[6] R. Athieno, *Empirical model in the characterization of High Frequency propagation in the Arctic region*. PhD thesis, University of New Brunswick., 2017.

[7] M. Abdullah, H. J. Strangeways, and D. M. Walsh, "Improving ambiguity resolution rate with an accurate ionospheric differential correction," *The Journal of Navigation*, vol. 62, no. 1, p. 151, 2009.

[8] N. Ya'acob, N. Tajudin, M. S. A. Remly, D. M. Ali, S. S. Sarnin, and N. F. Naim, "Observation of ionosphere scintillation and total electron content (tec) characteristic at equatorial region," in *Journal of Physics: Conference Series*, vol. 1152, p. 012020, IOP Publishing, 2019.

[9] M. S. Bagiya, H. Joshi, K. Iyer, M. Aggarwal, S. Ravindran, and B. Pathan, "Tec variations during low solar activity period (2005–2007) near the equatorial ionospheric anomaly crest region in india," in *Annales Geophysicae*, vol. 27, pp. 1047–1057, Copernicus GmbH, 2009.

[10] C. M. Candido, I. S. Batista, V. Klausner, P. M. de Siqueira Negreti, F. Becker-Guedes, E. R. de Paula, J. Shi, and E. S. Correia, "Response of the total electron content at brazilian low latitudes to corotating interaction region and high-speed streams during solar minimum 2008," *Earth, Planets and Space*, vol. 70, no. 1, pp. 1–19, 2018.

[11] A. Adewale, E. Oyeyemi, P. Cilliers, L. McKinnell, and A. Adeloye, "Low solar activity variability and iri 2007 predictability of equatorial africa gps tec," *Advances in space research*, vol. 49, no. 2, pp. 316–326, 2012.

[12] B. Oryema, E. Jurua, F. D'ujanga, and N. Ssebiyonga, "Investigation of tec variations over the magnetic equatorial and equatorial anomaly regions of the african sector," *Advances in Space Research*, vol. 56, no. 9, pp. 1939–1950, 2015.

[13] D. Hui, *Altitudinal variability of quiet-time plasma drifts in the equatorial ionosphere*. Utah State University, 2015.

[14] E. Yigit, *Atmospheric and Space Sciences: Ionospheres and Plasma Environments: Volume 2*. Springer International Publishing, 2018.

[15] K. Mohanakumar, *Stratosphere troposphere interactions: an introduction*. Springer Science & Business Media, 2008.

[16] M. Limberger, M. Hernández-Pajares, A. Aragón-Ángel, D. Altadill, and D. Dettmering, "Long-term comparison of the ionospheric f2 layer electron density peak derived from ionosonde data and formosat-3/cosmic occultations," *Journal of Space Weather and Space Climate*, vol. 5, p. A21, 2015.

[17] S. Schaer and S. helvétique des sciences naturelles. Commission géodésique, *Mapping and predicting the Earth's ionosphere using the Global Positioning System*, vol. 59. Institut für Geodäsie und Photogrammetrie, Eidg. Technische Hochschule . . . , 1999.

[18] R. Schunk and A. Nagy, *Ionospheres: physics, plasma physics, and chemistry*. Cambridge university press, 2009.

[19] L. F. McNamara, *The ionosphere: communications, surveillance, and direction finding*. Krieger publishing company, 1991.

[20] R. S. Fayose, R. Babatunde, O. Oladosu, and K. Groves, "Variation of total electron content [tec] and their effect on gnss over akure, nigeria," *Applied Physics Research*, vol. 4, no. 2, p. 105, 2012.

[21] S. Wyllie, *Modelling the temporal variation of the ionosphere in a Network-RTK environment*. PhD thesis, RMIT University, 2007.

[22] V. Chauhan, O. Singh, and B. Singh, "Diurnal and seasonal variation of gps-tec during a low solar activity period as observed at a low latitude station agra," *94.20. dv; 96.60. qd*, 2011.

[23] E. Astafyeva, I. Zakharenkova, and M. Förster, "Ionospheric response to the 2015 st. patrick's day storm: A global multi-instrumental overview," *Journal of Geophysical Research: Space Physics*, vol. 120, no. 10, pp. 9023–9037, 2015.

[24] R. Cop, S. Mihajlovic, and L. R. Cander, "Magnetic storms and their influence on navigation," *Pomorstvo, Journal of Maritime Studies*, vol. 22, no. 1, 2008.

[25] J. Gosling, D. McComas, J. Phillips, and S. Bame, "Geomagnetic activity associated with earth passage of interplanetary shock disturbances and coronal mass ejections," *Journal of Geophysical Research: Space Physics*, vol. 96, no. A5, pp. 7831–7839, 1991.

[26] R. Denton, K. Takahashi, I. Galkin, P. Nsumei, X. Huang, B. Reinisch, R. Anderson, M. Sleeper, and W. Hughes, "Distribution of density along magnetospheric field lines," *Journal of Geophysical Research: Space Physics*, vol. 111, no. A4, 2006.

[27] A. O. Olabode and E. A. Ariyibi, "Geomagnetic storm main phase effect on the equatorial ionosphere over ile–ife as measured from gps observations," *Scientific African*, vol. 9, p. e00472, 2020.

[28] N. V. Rao, T. Madhu, and K. L. Kishore, "Geomagnetic storm effects on gps aided navigation over low latitude south indian region," *IJCSNS Int. J. Comput. Sci. Network Secur*, vol. 10, pp. 37–42, 2010.

[29] J. S. Shim, *Analysis of total electron content (TEC) variations in the low-and middle-latitude ionosphere*. Utah State University, 2009.

[30] R. K. Mishra, B. Adhikari, N. P. Chapagain, R. Baral, P. K. Das, V. Klausner, and M. Sharma, "Variation on solar wind parameters and total electron content over middle-to low-latitude regions during intense geomagnetic storms," *Radio Science*, vol. 55, no. 11, p. e2020RS007129, 2020.

[31] M. Capderou, *Handbook of satellite orbits: From kepler to GPS*. Springer Science & Business, 2014.

[32] P. H. Dana, "Global positioning system (gps) time dissemination for real-time applications," *Real-Time Systems*, vol. 12, no. 1, pp. 9–40, 1997.

[33] E. D. Kaplan and C. Hegarty, *Understanding GPS/GNSS: principles and applications*. Artech house, 2017.

[34] B. Hofmann-Wellenhof, H. Lichtenegger, and E. Wasle, *GNSS–global navigation satellite systems: GPS, GLONASS, Galileo, and more*. Springer Science & Business Media, 2007.

[35] A. El-Rabbany, *Introduction to GPS: the global positioning system*. Artech house, 2002.

[36] G. Xu and Y. Xu, *GPS*. Springer, 2007.

[37] D. Sunehra, "Estimation of prominent global positioning system measurement errors for gagan applications," *European Scientific Journal*, vol. 9, no. 15, 2013.

[38] M. V. Codrescu, K. L. Beierle, T. J. Fuller-Rowell, S. E. Palo, and X. Zhang, "More total electron content climatology from topex/poseidon measurements," *Radio Science*, vol. 36, no. 2, pp. 325–333, 2001.

[39] A. Reznychenko, "Investigations of ionospheric disturbances using coherent hf instrumentation," Master's thesis, UiT Norges arktiske universitet, 2016.

[40] S. Kumar, E. L. Tan, and D. S. Murti, "Impacts of solar activity on performance of the iri-2012 model predictions from low to mid latitudes," *Earth, Planets and Space*, vol. 67, no. 1, pp. 1–17, 2015.

[41] M. Shehu, R. Said, and E. Okoro, "The trend of ionospheric total electron content near the equator," *Bayero Journal of Pure and Applied Sciences*, vol. 10, no. 1, pp. 258–264, 2017.

[42] N. Ya'acob, M. Abdullah, and M. Ismail, "Gps total electron content (tec) prediction at ionosphere layer over the equatorial region," *Trends in Telecommunications Technologies*, 2010.

[43] G. Seemala and C. Valladares, "Statistics of total electron content depletions observed over the south american continent for the year 2008," *Radio Science*, vol. 46, no. 5, 2011.

[44] F. Chu, J. Liu, H. Takahashi, J. Sobral, M. Taylor, and A. Medeiros, "The climatology of ionospheric plasma bubbles and irregularities over brazil," in *Annales Geophysicae*, vol. 23, pp. 379–384, Copernicus GmbH, 2005.

[45] J. Bittencourt, V. Pillat, P. Fagundes, Y. Sahai, and A. Pimenta, "Lion: A dynamic computer model for the low-latitude ionosphere," in *Annales Geophysicae*, vol. 25, pp. 2371–2392, Copernicus GmbH, 2007.

[46] M. Aggarwal, "Tec variability near northern eia crest and comparison with iri model," *Advances in space research*, vol. 48, no. 7, pp. 1221–1231, 2011.

[47] A. Brekke, *Physics of the upper polar atmosphere*. Springer Science & Business Media, 2012.

[48] E. Elemo, M. Ehigiator, and R. Ehigiator-Irughe, "Seasonal variations of the vertical total electron content (vtec) of the ionosphere at the gnss cor station (seerl) uniben and three other cors stations in nigeria," *Nigerian Journal of Technology*, vol. 37, no. 2, pp. 286–293, 2018.

[49] S. Oron, F. D'ujanga, and T. Ssenyonga, "Ionospheric tec variations during the ascending solar activity phase at an equatorial station, uganda," 2013.

[50] S. Bhattacharya, P. Purohit, and A. Gwal, "Ionospheric time delay variations in the equatorial anomaly region during low solar activity using gps," *94.20. dt; 92.70. Qr*, 2009.

[51] W. Gonzalez, J.-A. Joselyn, Y. Kamide, H. W. Kroehl, G. Rostoker, B. Tsurutani, and V. Vasyliunas, "What is a geomagnetic storm?," *Journal of Geophysical Research: Space Physics*, vol. 99, no. A4, pp. 5771–5792, 1994.

[52] S. Basu, S. Basu, F. Rich, K. Groves, E. MacKenzie, C. Coker, Y. Sahai, P. Fagundes, and F. Becker-Guedes, "Response of the equatorial ionosphere at dusk to penetration electric fields during intense magnetic storms," *Journal of Geophysical Research: Space Physics*, vol. 112, no. A8, 2007.

[53] B. G. Fejer, "Low latitude storm time ionospheric electrodynamics," *Journal of Atmospheric and Solar-Terrestrial Physics*, vol. 64, no. 12-14, pp. 1401–1408, 2002.

[54] N. Balan, L. Liu, and H. Le, "A brief review of equatorial ionization anomaly and ionospheric irregularities," *Earth and Planetary Physics*, vol. 2, no. 4, pp. 257–275, 2018.